

VILNIUS UNIVERSITY  
INSTITUTE OF BIOCHEMISTRY

Simona Povilonienė

**Investigation of amyloid fibrils forming proteins**

Summary of Doctoral Thesis  
Physical sciences, Biochemistry (04P)

Vilnius, 2011

This study was carried out at the Department of Molecular Microbiology and Biotechnology of the Institute of Biochemistry during 2006–2010.

Scientific Supervisor:

Dr. Vida Časaitė (Vilnius University Institute of Biochemistry, physical sciences, biochemistry – 04P).

**The thesis is defended at the Council of Biochemistry science direction of Vilnius University and Institute of Biochemistry:**

Chairman:

Prof. Dr. Habil. Valdas Stanislovas Laurinavičius (Vilnius University Institute of Biochemistry, physical sciences, biochemistry – 04P).

Members:

Prof. Dr. Habil. Vida Mildažienė (Vytautas Magnus University, physical sciences, biochemistry –04P).

Dr. Kęstutis Sužiedėlis (Vilnius University Institute of Oncology, biomedical sciences, biology –01B).

Assoc. Prof. Dr. Saulius Šatkauskas (Vytautas Magnus University, biomedical sciences, biophysics – 02 B).

Dr. Justas Barauskas (Vilnius University Institute of Biochemistry, physical sciences, biochemistry – 04P).

**Opponents:**

Assoc. Prof. Dr. Jolanta Sereikaitė (Vilnius Gediminas Technical University, physical sciences, biochemistry – 04P).

Assoc. Prof. Dr. Gintaras Valinčius (Vilnius University Institute of Biochemistry, physical sciences, biochemistry – 04P).

The doctoral thesis will be defended at the public meeting of the Council of Biochemistry at 11 a.m. on May 27, 2011 in the hall of the Institute of Biochemistry, Mokslininkų 12, Vilnius LT-08662, Lithuania.

Please send your comments to Scientific Secretary of VU Institute of Biochemistry, Mokslininkų 12, Vilnius LT-08662, Lithuania, Fax.: +37052729196, E-mail: [biochemija@bchi.vu.lt](mailto:biochemija@bchi.vu.lt).

The abstract of the dissertation was sent on April 27, 2011.

The thesis is available at the Library of the VU Institute of Biochemistry and the Library of Vilnius University.

VILNIAUS UNIVERSITETAS  
BIOCHEMIJOS INSTITUTAS

Simona Povilonienė

**Amiloidines fibriles formuojančių baltymų tyrimas**

Daktaro disertacijos santrauka  
Fiziniai mokslai, biochemija (04P)

Vilnius, 2011

Disertacija rengta 2006–2010 metais Vilniaus universiteto  
Biochemijos instituto Molekulinės mikrobiologijos ir biotechnologijos skyriuje.

Mokslinė vadovė:

dr. Vida Časaitė (Vilniaus universitetas Biochemijos institutas, fiziniai mokslai,  
biochemija – 04P).

**Disertacija ginama Vilniaus universiteto ir Biochemijos instituto biochemijos  
mokslo krypties taryboje:**

Pirmininkas:

prof. habil. dr. Valdas Stanislovas Laurinavičius (Vilniaus universitetas Biochemijos  
institutas, fiziniai mokslai, biochemija – 04P).

Nariai:

prof. habil. dr. Vida Mildažienė (Vytauto Didžiojo universitetas, fiziniai mokslai,  
biochemija –04P).

dr. Kęstutis Sužiedėlis (Vilniaus universitetas Onkologijos institutas, biomedicinos  
mokslai, biologija –01B).

doc. dr. Saulius Šatkauskas (Vytauto Didžiojo universitetas, biomedicinos mokslai,  
biofizika – 02 B).

dr. Justas Barauskas (Vilniaus universitetas Biochemijos institutas, fiziniai mokslai,  
biochemija – 04P).

Oponentai:

doc. dr. Jolanta Sereikaitė (Vilniaus Gedimino technikos universitetas, fiziniai mokslai,  
biochemija – 04P).

doc. dr. Gintaras Valinčius (Vilniaus universitetas, Biochemijos institutas, fiziniai  
mokslai, biochemija – 04P).

Disertacija bus ginama viešame Vilniaus universiteto Biochemijos mokslo krypties  
posėdyje, kuris įvyks 2011 m. gegužės mėn. 27d. 11 val. Biochemijos institute. Adresas:  
Mokslininkų 12, Vilnius LT-08662.

Disertacijos santrauka išsiųsta 2011 m. balandžio mėn. 27d.

Su disertacija galima susipažinti VU Biochemijos instituto ir Vilniaus universiteto  
bibliotekose.

## INTRODUCTION

The self-assembly of biomolecules is a powerful tool in the development of new nano-sized materials and devices (Zhao and Zhang, 2004). The construction of such functionalized nanomaterials with their own unique physical and chemical properties allow the innovations in the biomedical field developing various biosensors, electrochemical devices, medical products (Zhao and Zhang, 2004; Wang et al., 2009). Molecular self-assembly is widespread in nature, for example: lipids, surfactants, which form micelles and other complex structures in water as well as multivalent viral and ribosomal assembly using a strategy of “bottom – up” (Zhao and Zhang, 2007).

Biological nano-sized building blocks can be nucleic acids (DNA and RNA), proteins, peptides, bacteriophages or plant viruses. These potential biological macromolecules are self-assembled nanostructures. Proteinaceous materials can be chemically modified and can be applied in the construction of nanosystems. Comparing with DNA, proteins are more chemically and biologically "flexible" materials. Moreover, the proteinaceous building blocks are heterogeneous. Among the developed nanoscale constructs, the nanotubes made from peptides occupy the largest part (Zhang et al., 2002; Gazit, 2007).

Currently, much attention is paid to amyloid proteins that are associated with neurodegenerative diseases. For their ability to form self-assembling structures – fibrils composed of  $\beta$ -sheets, amyloids became very attractive for the development of new nanomaterials (Harrison et al., 2007). These materials serve as model systems providing fundamental understanding of structure-property relationships at the nanoscale (Wang et al., 2009).

The construction of new recombinant proteins as well as the creation of mutant and hybrid nanobiomolecular derivatives, based on amyloid fibrils forming proteins and peptides, provide the possibility to study the regularities of self-assembly and the conditions influencing fibrillization.

### **Aim of the dissertation work:**

The aim of the research was to construct novel recombinant proteins, to study hybrid nanobiomolecular structures they compose. The following tasks had been formulated:

- to construct A $\beta$ 40 and  $\alpha$ -Syn mutants and to study their ability to form  $\beta$ -sheet structures. To investigate the fibrillization conditions and properties of A $\beta$ 40 and  $\alpha$ -Syn mutant peptides;
- to study the possibilities of functional modification of A $\beta$ 40 and  $\alpha$ -Syn mutants;
- to determine whether histidines in A $\beta$ 40 sequence are crucial for heme binding;
- to construct hybrid proteins with self-assembling domain and to study their characteristics;
- to clone equine lysozyme gene and to express it in *E. coli* cells, to study the ability of recombinant lysozyme to form  $\beta$ -sheet fibrils.

### **Scientific novelty:**

Amyloid-forming peptides are most commonly associated with a number of neurodegenerative diseases, but they show enormous potential as templates for the fabrication of nanoscale materials. The ability to obtain unique materials with novel electronic, optical, catalytic and mechanical properties is the most promising perspective. The aim of this research work was to study hybrid nanoobjects based on A $\beta$ 40 and  $\alpha$ -Syn. These nanoconstructs could form fibrils and show special activity. For this purpose, new mutant and hybrid proteins based on the A $\beta$ 40 peptide and  $\alpha$ -Syn protein sequences were constructed. All the constructed mutant and hybrid proteins formed fibrillar structures of different morphology under appropriate conditions. By modifying A $\beta$ 40cys mutant peptides, it was demonstrated that gold nanoparticles positively influenced the aggregation of A $\beta$ 40 mutant.

It was also demonstrated that His residues in the A $\beta$ 40 sequence are responsible for heme binding. To elucidate that, mutants of hybrid Trx-A $\beta$ 40 protein, in which all the His residues were replaced by other amino acids, were constructed. Moreover, the complex of Trx-A $\beta$ 40 and heme was also a peroxidase.

$\alpha$ -Syn protein was also used for the construction of nanostructures. To investigate the possibilities of fibril modification  $\alpha$ -Syn<sub>cys141</sub> mutant was constructed.  $\alpha$ -Syn<sub>cys141</sub> mutant was fibrillized and modified with biotin and neutravidin conjugated gold nanoparticles. It is known that some  $\alpha$ -Syn based mutants were constructed and, prior to fibrillization, modified with chemical groups (Yushchenko et al., 2010). Nevertheless, there are no reports regarding fibril modification. Herein, was shown that  $\alpha$ -Syn<sub>cys141</sub> mutant is able to self-assemble into fibrils and can be modified with biotin and gold nanoparticles conjugated with neutravidin.

The production of active recombinant EL in bacterial cells, which was described herein, had been never reported before. Several high expression plasmids and protein purification procedures had been developed. It had been reported that EL was expressed in filamentous fungi *Aspergillus niger* (Spencer et al., 1999); however, purification of the recombinant protein was complicated due to the presence of fungal pigments. To avoid the purification problems, *E. coli* was chosen as a host for the production of large quantities of recombinant protein. Fibrillization studies showed that recombinant EL formed analogous structural elements as in the case of a native protein.

### **Defensive statements:**

- A $\beta$ 40 and  $\alpha$ -Syn mutants are capable of forming fibrillar structures and can be modified with functional groups.
- Hybrid proteins composed of A $\beta$ 40,  $\alpha$ -Syn and other proteins (PQQ-GDH, streptavidin and hydrophobin) form distinct fibrillar structures and can be applied to build nanosystems.
- His residues in the A $\beta$ 40 sequence are responsible of binding heme; the Trx-A $\beta$ 40 and heme complex acts as a peroxidase.
- EL can be expressed in *E. coli* cells and it self-assemble into fibrillar structures similar to the fibrils formed by native EL.

**Dissertation contents:**

The dissertation is written in Lithuanian and contains the following parts: Introduction, Literature review, Materials and Methods, Results and Discussion, Conclusions, List of References (206 positions), List of publications, Tables (2) and Figures (58). Total 140 pages.

## MATERIALS AND METHODS

**Reagents:** Acetonitrile (ACN) was purchased from Riedel-de Haën, Germany. Acetic acid and potassium chloride were from Achema, Czech Republic. Agarose and chloramphenicol were from Serva, Germany. Ammonium acetate, gold nanoparticles, EDTA, ethidium bromide, potassium acetate, sodium dodecylsulfate (SDS), tetramethylbenzidine (TMB), Tris-HCl, and biotin-maleimide were from Sigma, USA. Ampicillin was from Actavis, Denmark. Trypton bacto and  $\beta$ -mercaptoethanol were from Ferak, Germany. Brain Heart Infusion (BHI), Nutrient Agar (NA), and Nutrient Broth (NB) were from Oxoid, Great Britain.  $\text{CaCl}_2$  was from Penta, Czech Republic. Dimethylformamide (DMF), NaOH, and Trifluoroacetic acid (TFA) were from Merck, Germany. Ethyl alcohol was from Vilniaus Degtinè, Lithuania. Acrodisc Syringe filters were from Pall Corporation, USA. Glycerol was from Lachner, Czech Republic. Guanidine hydrochloride, Imidazole, Urea, and ThioflavinT (ThT) were from Fluka, Germany. HiTrap CM FF column, HiTrap<sup>TM</sup> Chelating HP column (1 ml or 5 ml), and Sepharose SP FF column were from GE Healthcare, Great Britain. Kanamycin was from AppliChem, Germany. Yeast extract was from Becton, Dickinson and company, France. Millipore dialysis filters Type VS and VSWP 0,025  $\mu\text{m}$  were from Millipore, USA. Sodium chloride (NaCl) was from Chempur, Poland. 10 nm Gold nanoparticles conjugated with neutravidin molecules were from Nanopartz, USA. Primers were from Metabion, Germany. Restriction and ligation enzymes, IPTG, PCR reaction enzymes, and GeneJET<sup>TM</sup> Plasmid Miniprep Kit were purchased from Fermentas, Lithuania.

**Bacteria and Plasmids:** *Escherichia coli* DH5 $\alpha$  strain ( $\phi 80\text{dlacZ}\Delta\text{M15 } \Delta(\text{lacZY-argF})\text{U169 } \text{deoR } \text{recA1 } \text{endA1 } \text{hsdR17}(\text{r}_\text{K}^- \text{m}_\text{K}^+) \text{ sup } \text{E44 } \text{thi-1 } \text{gyrA96 } \text{relA1}$ ) was purchased from Pharmacia (USA). *Escherichia coli* BL21(DE3) ( $\text{F}^- \text{ompT } \text{gal } \text{hsdS}_\text{B}(\text{r}_\text{B}^- \text{m}_\text{B}^-) \text{ dcm } \text{lon}$  (DE3)) and Rosetta (DE3)pLysS ( $\text{F}^- \text{ompT } \text{hsdS}_\text{B}(\text{R}_\text{B}^- \text{m}_\text{B}^-) \text{ gal } \text{dcm } \lambda(\text{DE3} [\text{lacI } \text{lacUV5-T7 } \text{gene 1 } \text{ind1 } \text{sam7 } \text{nin5}]) \text{ pLysSRARE}(\text{Cam}^\text{R})$ ) strain were purchased from Avidis France.

Plasmids pET3a-*trx-a $\beta$ 40*, pET3a-*trx-a $\beta$ 40cys2*, pET3a-*trx-a $\beta$ 40cys39*, pET3a-*casp7* were a gift from Dr. Anders Olofsson. Plasmids pETM-11, pETM-50, pETM-52, pETM-80, pETM-82 were a gift from Dr. Gunter Stier. pET28-EL was a gift from Dr. Mantas Mališauskas. pRK172 was a gift from Dr. L.A. Morozova-Roche, pUC57-*sha* and pUC27-*sa* were purchased from GenScript Corporation (USA). pASKIBA3-PT15 (Meissner et al., 2004) and pET-11M-yli1 (Southall et al., 2006).

Plasmids pET3a-*trx-a $\beta$ 40H6A*, pET3a-*trx-a $\beta$ 40H6S*, pET3a-*trx-a $\beta$ 40H6C*, pET3a-*trx-a $\beta$ 40H13A*, pET3a-*trx-a $\beta$ 40H14A*, pET3a-*trx-a $\beta$ 40H6/13A*, pET3a-*trx-a $\beta$ 40H6/14A*, pET3a-*trx-a $\beta$ 40H6/13/14A*, pET21d-*sa-a $\beta$ 40*, pET21b-*sa-hfb-a $\beta$ 40*, pTabpvu16, pTabecol1, pET21 $\alpha$ -Syn, pET21 $\alpha$ -Syncys141, pTsyneco, pETM11-EL, pYliab9 and pYliab10 were constructed in this work.

**Preparation of Media:** Different media were prepared as follows:

BHI: 37g BHI 1L H<sub>2</sub>O; SOB media: 20 g/L Trypton-Bacto, 5 g/L Yeast extract, 0.6 g/L NaCl, 0.19 g/L KCl, 10 ml/L 1M MgCl<sub>2</sub>, 10 ml/L 1M MgSO<sub>4</sub>; NA media: 28 g NA 1 L H<sub>2</sub>O; NB: 13 g NB 1 L H<sub>2</sub>O; LB (Luria Bertoni): 10 g/L Trypton-Bacto, 5 g/L Yeast extract, 10 g/L NaCl, pH 7.0. All the media were autoclaved for 30 min at 121 °C temperature. Bacteria were cultivated on the solid media plates at 37 °C or in the liquid media at 30–37 °C with aeration.

**Plasmid DNA extraction:** Bacterial cells were grown overnight in the NB media containing appropriate antibiotic at 30 °C with aeration. The biomass was harvested by



centrifugation for 10 min at 4000 g 4 °C. To isolate plasmid DNA, the alkaline lysis/phenolic extraction procedure was applied (Sambrook et al., 1989). For rapid plasmid DNA extraction, GeneJET™ Plasmid Miniprep Kit (Fermentas) was used.

**PCR reaction:** The recombinant *Taq* DNA or *Pfu* polymerases with appropriate buffers and supplements or 2X PCR Mix were used according the recommendations of the manufacturer (Fermentas). PCR was performed with *Mastercycler personal* and *Mastercycler ep* gradient S PCR devices (Eppendorf).

**Digestion of DNA with Restriction Endonucleases:** DNA was digested according the recommendations of manufacturer (Fermentas). DNA was incubated with appropriate restriction endonucleases for 15–60 min at recommended temperature.

**DNA electrophoresis in agarose gels:** Horizontal DNA electrophoresis was performed using agarose gels 1% in TAE buffer as described by Sambrook and co-workers (Sambrook et al., 1989) Gels were stained with ethidium bromide and analyzed by UV using Herolab Transilluminator UVT–28ME (Germany). The molecular mass of DNA fragments was determined with Gene Ruler™ DNA ladder Mix (Fermentas).

**DNA extraction from agarose gels:** In this work, DNA Extraction Kit (Fermentas) was used. Procedure was performed according the manufacturer protocol.

**DNA Ligation:** The mixture of insert DNA, linearized vector, T4 DNA Ligase Buffer and T4 DNA Ligase was prepared and incubated at 22 °C for 1–2 hours. Ligase was inactivated by heating the mixture at 65 °C for 10 min and then cooled.

**The preparation of competent cells and the conditions of electroporation:** *E. coli* cells were inoculated into the 5 mL of BHI medium and cultivated overnight at 30 °C temperature with aeration. The competent cells were prepared according the procedure described by (Sharma and Schimke, 1996).

**Determination of nucleotide sequence:** Plasmid DNA was purified as described in the chapter above. The concentration of DNA was determined by electrophoresis in agarose gel, using Mass Ruler™DNA Ladder (High Range) markers (Fermentas). The nucleotide sequences were determined at the Sequencing Centre in the Institute of Biotechnology, Vilnius. BigDye® Terminator v3.1 Cycle sequencing Kit (Applied Biosystems) and Standard sequencing M13/pUC primers were used. The chromatograms of sequencing were analyzed with *Chromas 2.24* program (<http://www.technelysium.com.au/chromas.html>) and *Vector NTI Advance™ 9.0* program. The alignments of sequences were performed with BLAST tools (<http://www.ncbi.nlm.nih.gov/blast/Blast.cgi>).

**Preparation of free-cell extracts:** *E. coli* cells were transformed with plasmids and cultivated on the NA plates with appropriate antibiotic. 1:50 of overnight culture was transferred to 1 L of NB with ampicillin and were grown at 30 °C or 37 °C with aeration until the OD<sub>600</sub> of the culture reached 0.6–0.8. Then 0.1–0.5 mM IPTG was added to the medium and cultivation was continued for 6–20 h. The cells were harvested by centrifugation and washed with 50 mM Tris-HCl pH 8.5 and again centrifuged. Washed cells were resuspended in the same buffer and disrupted by sonification (2 min 22 kHz, in ice-water bath). The cell debris was separated by centrifugation (4000 g 60 min). If protein was expressed in the inclusion bodies, the cells debris with insoluble bodies was solubilized in the same buffer containing 6 M Urea.

**Protein analysis in SDS-PAGE** was performed in the slab gels containing 10–20 % acrylamide for the separating gel and 5 % acrylamide for the stacking gel. Gels were stained with PageBlue™ Protein Staining Solution (Fermentas) Unstained Protein

Molecular Weight Marker (14.4–116) and PageRuler™ Prestained Protein Ladder 10–170 kDa) (Fermentas) molecular weight standards were used. The procedure was done as recommended by the manufacturer.

**Purification of proteins:** Cells were harvested by centrifugation and disrupted by sonication. The cell free extract was loaded on the chelating (Ni) column. The Loading buffer: 50 mM Tris-HCl 0.1 M NaCl, 5 % glycerol, pH 8.5; Elution buffer: 50 mM Tris-HCl, 0.1 M NaCl 5 % glycerol and 0.5 M imidazole, pH 8.5. The collected fractions with fused proteins were analyzed in the 15 % SDS-PAGE and then dialyzed against the loading buffer.

**Protein purification from the inclusion bodies:** The cell debris with inclusion bodies was resuspended in the buffer: 50 mM Tris-HCl, 0.1 M NaCl, 0.5 M Urea, pH 8.5, and centrifuged (10000 *g* 60 min). The supernatant was discarded, and inclusion bodies were dissolved in the buffer containing: 50 mM Tris-HCl, 0.1 M NaCl, 6.0 M Urea, pH 8.5. The solution was centrifuged and the clear extract was loaded on the chelating (Ni) column. Loading buffer: 50 mM Tris-HCl, 0.1 M NaCl, 6.0 M Urea, pH 8.5; Elution buffer: 50 mM Tris-HCl, 0.1 M NaCl, 6.0 M Urea, 500 mM imidazole, pH 8.5. The collected fractions were dialyzed against buffer: 50 mM Tris-HCl, 0.1 M NaCl, pH 8.5 and analyzed in the 15 % SDS-PAGE.

**The expression and purification of caspase7:** Strain *E. coli* Rosetta was transformed with the plasmid pET3a-*casp7* harboring gene encoding caspase7. The culture was grown at 30 °C, until OD<sub>600</sub> reached 0.3–0.4 then temperature was reduced to 24 °C and cells were grown until OD<sub>600</sub> reached 0.6–0.8 and 0.4 mM IPTG were added and grown for 18 h. The biomass was harvested, disrupted, and purified as was described above.

**The digestion of fused proteins with caspase7:** The fused Trx-Aβ proteins were digested with purified caspase7. The reaction mixture was: 20 mM 2-ME, 5 mM CaCl<sub>2</sub>, protein:caspase7 at different proportions 1:1, 1:2, 1:5, 1:10, 1:20, and incubated at 37 °C for 10 h.

**The purification of Aβ peptides:** After digestion with caspase7, the mixture of proteins was analyzed in the 18 % PAGE. Then 6.0 M guanidine-HCl were added to the mixture to dissolve any of precipitates. The clear solution was filtrated with Acrodisc Syringe filters and then loaded onto the reverse phase column (RPC15 3 mL). The column was precalibrated with 10 volumes of loading buffer: 0.05% TFA and 5% acetonitrile (ACN), then the protein solution was loaded, the column was prewashed with two column volumes of loading buffer and peptides were eluted by increasing the concentration of elution buffer: 0.05% TFA and 95% ACN (total volume of elution buffer – 25 column volumes). The collected fractions were analyzed in 18 % SDS-PAGE and fractions with peptide were frozen at –80 °C and lyophilized for 12 h. Peptides were dissolved in the appropriate buffers.

**The construction, expression, and purification of mutant fused Trx-Aβ40 proteins:** The mutants were obtained by site-directed mutagenesis. Site-directed mutagenesis of Trx-Aβ40 was performed by PCR amplification of pET3a-*trx-aβ40* using *Pfu* polymerase. The different pairs of primers were used to amplify fused gene of thioredoxin and Aβ40 with introduced mutations. In the first step, two separate PCRs were carried out to generate the primary PCR products, having overlapping ends (mutating primer (F) and flanking primer (R) in one tube and mutating primer (R) and flanking primer (F) in the second tube). PCR products were then used as templates to

generate the full-length sequence. Flanking primers were designed with the recognition sites of restriction endonucleases *Xba*I and *Bam*HI.

The amplified and *Xba*I-*Bam*HI digested fragments were ligated into vector pET3a and subsequently transformed into competent DH5 $\alpha$  cells. Positive clones were screened and DNA sequencing (In the Sequencing Centre, Institute of Biotechnology) confirmed plasmids containing fused *trx-a $\beta$ 40* gene with certain mutations.

The mutant variants of fused Trx-A $\beta$ 40 proteins were expressed and purified in the same way as the fused Trx-A $\beta$ 40 proteins.

**The construction, expression and purification of fused A $\beta$ 40, hydrophobin and streptavidin proteins:** The constructs of genes *tsa-a $\beta$ 40* and *msa-hfb-a $\beta$ 40* were cloned in the expression vectors pET21d and pET21b respectively. Plasmid pUC57-*tsa-a $\beta$ 40* was digested with *Nco*I and *Xho*I, obtained fragment was cloned into the pET21d vector digested with the same restriction endonucleases. Plasmid pUC57-*tsa-hfb-a $\beta$ 40* was digested with *Bam*HI or *Hind*III. The obtained fragment was cloned into the pET21b digested with the same restriction endonucleases.

*E. coli* DH5 $\alpha$  strain was transformed with newly constructed plasmids pET21d-*sa-a $\beta$ 40* and pET21b-*sa-hfb-a $\beta$ 40*. The positive clones were analyzed by PCR using primers T7Pro and T7Ter and by the digestion with appropriate restriction enzymes' combination. DNA sequencing confirmed plasmids containing genes encoding fused proteins. The expression and purification of fused proteins were performed as described previously. The purified proteins were dialyzed against 20 mM ammonium hydrocarbonate buffer and lyophilized.

**The construction, expression, and purification of hybrid A $\beta$ 40 and GDH from *Acinetobacter* sp. protein:** GDH gene from *Acinetobacter* sp. is cloned into plasmid pASKIBA3-PT15. In the end of GDH encoding gene there are *Eco*47III recognition site (in the C terminal of GDH encoding part) and *Pvu*II recognition site (in the middle of the gene) that were used to insert A $\beta$ 40 encoding fragment. Amplified *a $\beta$ 40* gene was digested with *Ecl*136II and *Sna*BI restriction enzymes and cloned into *Pvu*II site of the pASKIBA3-pT15 plasmid (obtained plasmid pPTabpvu16) and into *Eco*47III site (obtained plasmid pPTabeco1). *E. coli* DH5 $\alpha$  strain was transformed with newly constructed plasmids. Bacteria were cultivated on the solid agar media at 37 °C overnight, then one colony was transferred into liquid NB media and were grown at 30 °C with aeration. After 6 h OD<sub>600</sub> reached 1.0 and culture was cooled to 25 °C, and promoter was induced by 1.0  $\mu$ M anhydrotetracycline (AHT) and continued cultivated at 30 °C for 20 h. The biomass was harvested by centrifugation, resuspended in the 50 mM Tris-HCl pH 8.0 buffer and disrupted by sonification. The fusion proteins were purified by Ion Exchange chromatography (CM FF column). Loading buffer: 50 mM Tris-HCl pH 7.5, Elution buffer: 50 mM Tris-HCl 1.0 M NaCl, pH 7.5. The purified proteins were dialyzed against 20 mM ammonium hydrocarbonate buffer, frozen and lyophilized.

**The construction, expression and purification of hybrid  $\alpha$ -Syn and GDH from *Acinetobacter* sp. protein:** To insert  $\alpha$ -Syn encoding gene into the GDH gene, *Eco*47III site was used, as described previously.  *$\alpha$ -syn* gene was amplified and digested with *Eco*RV and cloned into plasmid pASKIBA3-pT15 that had been previously cleaved with *Eco*47III (obtained plasmid pPTsyneco).

The induction and expression of hybrid GDH and  $\alpha$ -Syn protein were carried out as described above.

**The construction, expression, and purification of PQQ-GDH from *E. coli* and A $\beta$ 40 hybrid protein:** The gene encoding GDH from *E. coli* was in plasmid pET11M-*yli1*. There is only one *AjiI* target site that was used to clone A $\beta$ 40 gene. *a $\beta$ 40* gene was amplified, digested with *Ecl136II* and *SnaBI* and cloned into the plasmid pET11M-*yli1* that had been cleaved previously with *AjiI*. After the screening, two plasmids containing fused protein were selected (p*Yli-ab9* and p*Yli-ab10*). The expression and purification were carried out as described previously.

**The construction of mutant  $\alpha$ -Syn<sub>141</sub> protein:** pRK172 plasmid and primers T7Pro and Syn<sub>cys</sub>R were used to construct  $\alpha$ -Syn<sub>141</sub> mutant. Obtained PCR fragment was digested with *XbaI* and *XhoI* and ligated into pET21a vector that had been previously cleaved with *XbaI* and *XhoI*. *E. coli* DH5 $\alpha$  was transformed with ligation mixture. The positive clones were tested by PCR and restriction enzymes. DNA sequencing verified the mutation.

**The expression and purification of  $\alpha$ -Syn and  $\alpha$ -Syn<sub>141</sub> proteins:** *E. coli* BL21 (DE3) cells were transformed with pET21 $\alpha$ -Syn and pET21 $\alpha$ -Syn<sub>141</sub> plasmids. The cells were spread on NA plate with Ap 50  $\mu$ g/mL. The cells were cultivated at 37 °C until OD<sub>600</sub> reached 0.8, protein expression was induced by addition of 0.2 mM IPTG. The cells were grown at 30 °C and harvested after 4 h. The biomass was resuspended in the buffer: 50 mM Tris-HCl, 0.1 mM EDTA, 0.2 mM PMSF, pH 8.0 and disrupted by sonication. The mixture of disrupted cells was heated for 10 min at 100 °C, and then centrifuged. The clear extract was loaded onto Q XL 1 ml column (Loading buffer: 50 mM Tris-HCl, pH 7.5; Elution buffer: 50 mM Tris-HCl, 1.0 M NaCl, pH 7.5) (Der-Sarkassian et al., 2003). If protein was not pure, it was reloaded onto ANX column (loading buffer: 50 mM Tris-HCl, pH 7.5; elution buffer: 50 mM Tris-HCl, 1.0 M NaCl, pH 7.5). After purification, protein was analyzed in the 15 % SDS-PAGE.

**The cloning, expression and purification of equine lysozyme (EL):** EL encoding DNA fragment from the pET28a plasmid was cut out with *NcoI* and *NotI* and ligated into the pETM-11, pETM-50, pETM-52, pETM-80 and pETM-82 plasmids pre-cut with the same restriction endonucleases. The competent *E. coli* DH5 $\alpha$  cells were transformed with ligation mixtures. Positive clones were confirmed by DNA sequence analysis.

*E. coli* BL21 (DE3) or C43 (DE3) cells harboring the appropriate plasmid were used for the production of the recombinant protein. 10 mM of CaCl<sub>2</sub> were added to the medium when appropriate. Cultures were grown until late log-phase ( $A_{280}$  nm, 0.8) at 30 °C and the protein expression was induced with 0.5 mM IPTG. The cells were maintained at 30 °C for 5 h, harvested by centrifugation (4000 g, 20 min, 4 °C) and resuspended in 50 mM Tris-HCl, pH 8.5 and disrupted by sonication. Cell debris was collected by centrifugation (10000 g, 20 min, 4 °C). Insoluble inclusion bodies were solubilized in 6.0 M urea (in the same buffer) and applied to a nickel (Ni)-chelating affinity column (GE Healthcare) according to the manufacturer's instructions. Proteins were eluted with 500 mM imidazole; fractions containing His-tagged EL were pooled. Denatured proteins were refolded by dialysis against 20 mM Tris-HCl, 1 mM 2-mercaptoethanol (2-ME), 10 mM arginine, pH 8.0. After refolding, soluble proteins were separated by centrifugation. The tag was removed by cleavage with tobacco etch virus (TEV) protease for 3 h at room temperature. The cleaved protein was applied to a Sepharose SP FF column (GE Healthcare) equilibrated with 20 mM Tris-HCl, pH 8.0,

and EL was eluted with sodium chloride (NaCl) gradient (0–1 M). Fractions containing the pure EL were pooled, dialyzed against 20 mM ammonium hydrogen carbonate buffer, pH 7.5 and lyophilized. Protein concentration was determined using the Lowry method and spectrophotometrically at 280 nm, extinction coefficient 34 530 M/cm for EL.

**EL activity assay:** activity was measured at 25 °C in 50 mM Tris-HCl buffer, pH 7.5. The lysis of *Micrococcus luteus* cells (Sigma) (0.15 mg/ml) was monitored by measuring the decrease in absorbance at 450 nm over 30 s period (Kikuchi et al., 1988). One unit of lysozyme is defined as a change in 0.001 units of absorbance/min. Comparing with published information, we determined the lysozyme activity of HEWL (Fluka) under the same conditions.

**Interaction of heme and fusion proteins:** A stock solution of heme was prepared by freshly solved hemin in 0.1 M NaOH. The heme solution was diluted with PBS buffer (pH 9.0) obtaining concentration of 6 mM of heme. Solution must be kept in dark.

The concentrations of proteins were calculated according to absorbance at 280 nm wavelength (molar extinction coefficient = 15460). The formation of A $\beta$ -heme complex was determined by heme binding to A $\beta$  fusion proteins at a ratio 1:1 (the final concentration in PBS solution pH 7.5 was 6  $\mu$ M). The spectrum was measured between 350 and 750 nm. The peak at 380 nm was observed when heme bound to A $\beta$  fusion proteins (Atamna and Boyle, 2006).

**Peroxidase activity of the A $\beta$  fusion protein-Heme complex:** Peroxidase activity of the A $\beta$  fusion protein-heme complex was measured by the oxidation of TMB (3,3',5,5'-Tetramethylbenzidine) by H<sub>2</sub>O<sub>2</sub> following the increase in absorbance at 652 nm every 5 and 10 minutes. The peroxidase activity of A $\beta$  fusion protein-heme was tested in the concentration of 1.2  $\mu$ M in PBS solution pH 7.5.

**The formation of fibrils:** Depending on proteins and peptides, different fibrillization assays were applied. Proteins and peptides were dissolved in the appropriate buffers (pH 2.0–8.0) and fibrillized at 37 °C or 57 °C, agitating by 550 rpm or without agitation, 3–10 days or 6 months, when protein concentration was 1–10 mg/ml. 0.01% of NaN<sub>3</sub> was added to the solution.

Approximately 10 mg/ml or 1 mg/ml of EL was dissolved in 10 mM sodium acetate buffer, pH 4.5, containing 0.01% NaN<sub>3</sub> with or without 10 mM CaCl<sub>2</sub> and incubated at 50–55 °C for 3–5 days.

**Thioflavine T-binding assay:** Fluorescence emission spectra of Thioflavine T (ThT), excited at 450 nm, were recorded between 460 and 600 nm on a PerkinElmer precisely LS55 luminescence spectrometer using excitation and emission bandwidths of 5 nm. Fibril formation was monitored by adding aliquots of protein fibril solutions to a final concentration 5  $\mu$ M to 1 ml of a 5  $\mu$ M ThT solution (LeVine, 1993).

**Atomic force microscopy:** A small amount (typically 1  $\mu$ L) of the solution was put on mica surface lying horizontally. Typically, the liquid was spread over the whole area under the weight of the top plate. The immobilization time varied from 5 to 20 min. The density of the surface objects was increased or decreased by the immobilization time. Surrounding temperature was about 23 °C and the relative humidity of the air was about 45%. The surfaces were rinsed in distilled water after the separation. The samples were dried before the surface analysis. Surfaces of the samples were visualized by scanning probe microscope SPM D3100/Nanoscope IVa (Veeco). The surfaces were typically

scanned by the SPM in standard contact and tapping AFM modes. The images were processed by the Nanoscope software (Veeco).

**The modification of amyloid fibrils with biotin:** 4.5 mg of biotin maleimide were dissolved in 200  $\mu$ L of DMSO and then dilute with 50 mM sodium phosphate buffer (the initial concentration of solution 10 mM). For biotinylation 5 molar excess of biotin maleimide to protein concentration is needed. Prior to biotinylation, proteins were reduced with 1 mM of TCEP and dialyzed. After biotinylation, proteins were dialyzed against appropriate buffer.

**TEM analysis:** 1  $\mu$ L of modified fibril solution was mounted on a carbon-coated palladium grid (400 mesh) The sample was dried at room temperature for 5–10 min and subsequently negatively stained with 2% aqueous uranyl acetate solution (Reachim, Russia) and dried with filter paper. Sample grids were viewed in a transmission electron microscope (JEOL-JEM-100S transmission electron microscope, Japan). Instrumental magnification x 25000. The dimensions of the fibrils were obtained directly from the micrographs.

**The determination of tetrameric streptavidin activity:** Tetrameric streptavidin activity was tested with biotin conjugated with stilbazole fluorophore (chemical formula  $C_{37}H_{55}ClN_4O_6S$ , molecular mass 719.37 g/mol). The excitation of this compound is 479 nm and emission is recorded at 594 nm. The samples with streptavidin were mixed with 5 molar excess of biotin-stilbazole and analyzed in the 15 % PAGE in semi-denaturing conditions. After electrophoresis, the gel was analyzed under UV. The interaction of streptavidin and stilbazole-biotin was confirmed by determining the fluorescent spots in the position of streptavidin protein.

**The modification of A $\beta$ 40cys2 and A $\beta$ 40cys39 peptides by gold nanoparticle:** 5  $\mu$ L of 0.01% HAuCl<sub>4</sub> were added before and after fibrillization to a final concentration 0.0025%.

## RESULTS AND DISCUSSION

A $\beta$  peptides,  $\alpha$ -Syn and EL are known to form fibrillar structures *in vivo* and *in vitro*. The aim of this study was to investigate the properties of proteins that form amyloid fibrils and to test the possibilities to apply these proteins as building blocks of nanostructures.

### INVESTIGATION OF AGGREGATION OF A $\beta$ 40 PEPTIDE DERIVATIVES

**Construction and purification of A $\beta$ 40 derivatives.** The purification of A $\beta$  peptides was a three step process. Firstly, the hybrid Trx-A $\beta$ 40 protein was expressed and purified, then it was digested with caspase7, and finally A $\beta$ 40 peptide was purified by RPC. pET3a-*trx-a $\beta$ 40* plasmid harboring *trx* and *a $\beta$ 40* genes, which were separated with DNA fragment encoding oligopeptide (DEVD) – a target of caspase7.

After the expression of hybrid Trx-A $\beta$ 40 protein in *E. coli* BL21 (DE3) cells, SDS-PAGE analysis showed that 50 % of protein formed inclusion bodies (was insoluble) when cells were cultivated at 30 °C, and ~90 % of protein formed inclusion bodies when grown at 37 °C.

Insoluble hybrid protein was collected and purified under denaturing conditions. An 18 kDa band (theoretical molecular mass of Trx-A $\beta$ 40 protein is 18159.53 g/mol) was observed in SDS-PAGE (Fig. 1). About 10 mg of protein could be obtained from one liter of culture.

Caspase7 was expressed and purified as described in methods, and used for the proteolysis of hybrid Trx-A $\beta$ 40 protein. The most optimal hydrolysis was performed at 37 °C for 12 h when reaction mixture contained caspase 1:5 protein (Fig. 1). Since some of proteins precipitated, the hydrolyzate of protein was dissolved with guanidine-HCl and loaded onto RPC column. A $\beta$ 40 peptide eluted when ACN concentration was about 40%. The yield of A $\beta$  peptide was 1 mg from 1L of culture.

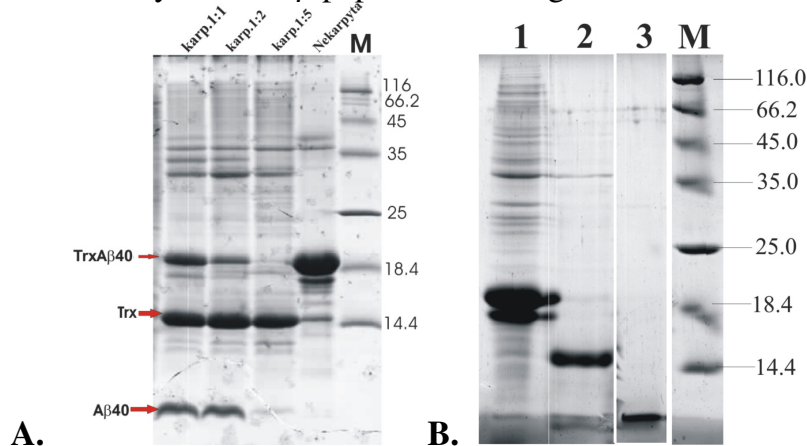


**Fig. 1.** The electrophoretic view of hydrolyzed Trx-A $\beta$ 40 proteins (A). Electrophoretic view of A $\beta$ 40 peptides after the purification with RPC (B): 1 – Trx-A $\beta$ 40, 2 – Trx, 3 – A $\beta$ 40, M – mass ruler.

Mutant A $\beta$ 40cys2 and A $\beta$ 40cys39 were expressed and purified in the same way as A $\beta$ 40 mutant. The yield of mutant peptides was ~1 mg from 1 L of culture.

#### Investigation of self-assembling $\beta$ -sheet structures formed by A $\beta$ 40 mutants

Higher temperature, prolonged incubation, higher concentration of protein, acidic pH were applied for the fibrillization of proteins based on A $\beta$ 40 sequence. The fibrillar samples of A $\beta$ 40cys2, A $\beta$ 40cys39 were prepared in neutral and acidic pH (pH 7.5 (50 mM Tris-HCl), peptide concentration 1 mg/ml, 37 °C, 5 days, 550 rpm, 0.01% NaN<sub>3</sub>, ( hereinafter referred to as neutral conditions); pH 3.0 (100 mM Glycine-HCl), peptide concentration 1 mg/ml, 57 °C 5 days, 550 rpm, 0.01% NaN<sub>3</sub>, ( hereinafter referred to as acidic conditions)). A $\beta$ 40 peptide was purified and fibrillized in the same manner as mutant A $\beta$ 40cys2, A $\beta$ 40cys39 peptides and was used as a control sample to evaluate the differences of fibril structures that previously were evaluated by measuring the increase of ThT fluorescence (Fig. 2).

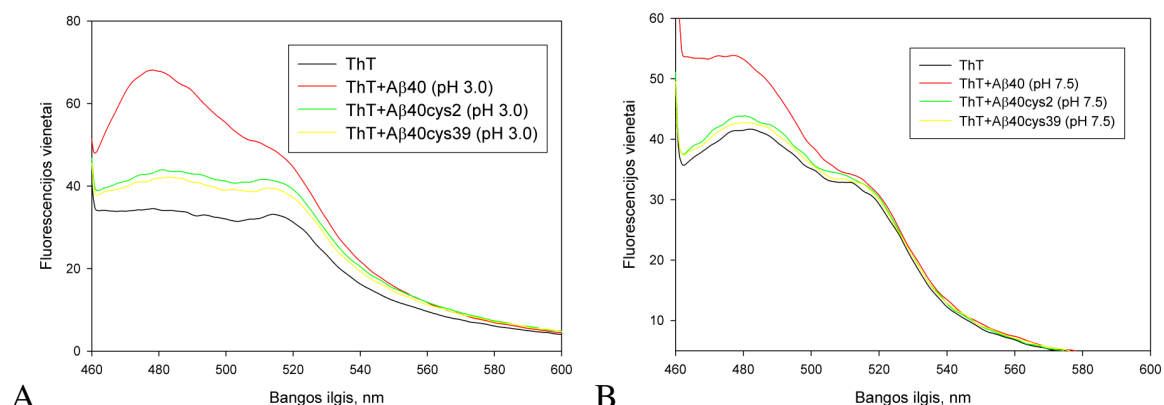


**Fig. 2.** The ThT fluorescence spectra with A $\beta$ 40, A $\beta$ 40cys2 and A $\beta$ 40cys39 fibril samples obtained after the fibrillization at acidic (A) and neutral pH (B).

The results of spectra showed that A $\beta$ 40 peptide formed more fibrils than mutant A $\beta$ 40cys peptides. A $\beta$ 40cys2 was more prone to form fibrils than A $\beta$ 40cys39.

The morphology of fibrils formed by A $\beta$ 40 and its mutants, obtained under acidic conditions, was evaluated by AFM *ex situ* tapping mode (Fig. 3).

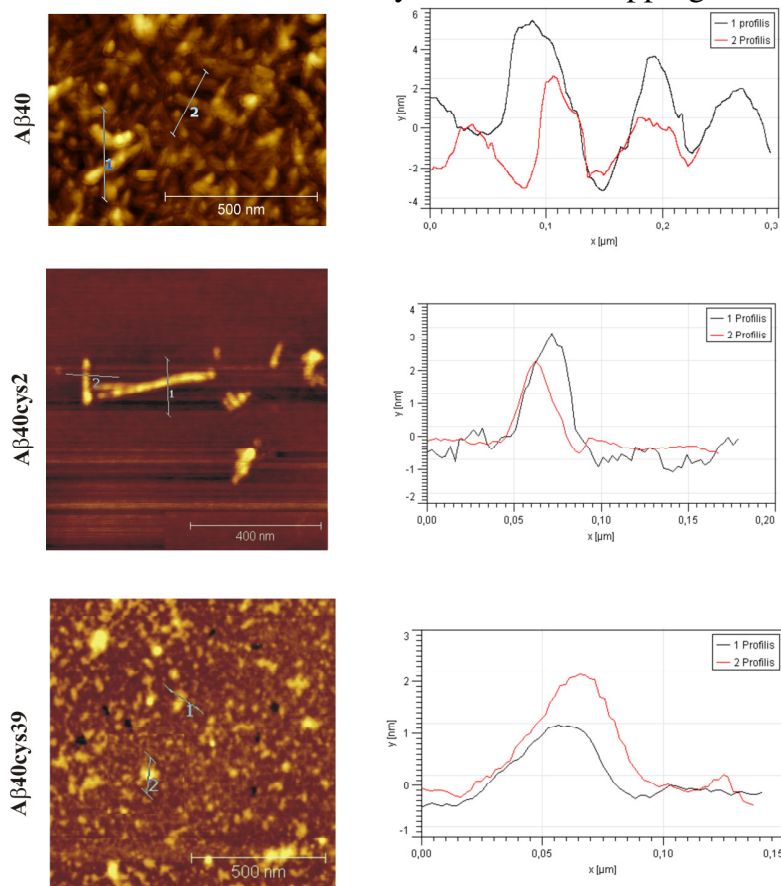


**Fig. 3.** The AFM *ex situ* images of A $\beta$ 40, A $\beta$ 40cys2 and A $\beta$ 40cys39 fibrils. Topography images are shown on the left and cross-section profiles on the right. Scale and profiles are marked with white bars. The scanning field selected randomly.

The ThT and AFM results showed that A $\beta$ 40cys2 and A $\beta$ 40cys39 peptides were less prone to form fibrils than A $\beta$ 40 at pH 3. At pH 7.5, peptides formed less fibrils (Fig. 2B). AFM analysis demonstrated that A $\beta$ 40 peptide formed fibrils (Fig. 3) from 3.5 to 9.0 nm in height, of medium length, unbranched structures. A $\beta$ 40cys2 fibrils remained long and unbranched structures, and the height of the fibrils varied 2.0–7.0 nm. A $\beta$ 40cys39 fibrils formed structures that were 1.5–3.0 nm in height, which differed in morphology from the fibrils formed by other two peptides.

### Investigation of interaction between hybrid Trx-A $\beta$ 40 and Heme

Trx-A $\beta$ 40 mutants with altered His codons in A $\beta$ 40 sequence were used for the analysis of interaction with heme. Trx-A $\beta$ 40 mutants, with all His residues in A $\beta$ 40 sequence altered with other amino acids, were constructed by carrying out site-directed mutagenesis. 10 mutant plasmids were obtained (1 table).

**Table 1. Trx-A $\beta$ 40 mutants with altered His codons in the A $\beta$ 40 sequence.**

	His codon	Altered codon	The name of mutant
<b>Mutants</b>			
<b>Single:</b>	6 His	6 Ala	H6A
		6 Ser	H6S
		6 Cys	H6C
	13 His	13 Ala	H13A
		13 Cys	H13C
	14 His	14 Ala	H14A
<b>Double:</b>	13-14 His	13-14 Ala	H(13-14)A
	6/13 His	6/13 Ala	H(6/13)A
	6/14 His	6/14 Ala	H(6/14)A
<b>Triple</b>	6/13-14 His	6/13-14 Ala	H(6/13-14)A



The expression level of Trx-A $\beta$ 40 mutants was lower, especially in the case of triple mutant, than Trx-A $\beta$ 40, and all the mutant proteins were expressed in inclusion bodies.

The spectra of heme binding showed that all mutant proteins bound heme with different intensity. The interaction of heme and mutant proteins was at least several times weaker than interaction between heme and Trx-A $\beta$ 40. The weakest interaction was observed between heme and triple mutant H(6/13-14)A. The strongest interaction with heme and mutants was observed with single H6A and H6C mutants. The results substantiated the hypothesis that His is important in binding iron atom of heme in A $\beta$ 40 sequence. Hybrid Trx-A $\beta$ 40 protein had additional histidines. Trx with 6 His-tag also interacted with heme, but this interaction was weak (data not shown).

It was demonstrated that Trx-A $\beta$ 40 could bind heme and formed complex could function as peroxidase. The peroxidase activity of Trx-A $\beta$ 40+heme complex was measured by the oxidation of TMB by H<sub>2</sub>O<sub>2</sub> by following the increase in absorbance at 652 nm (Fig. 5).

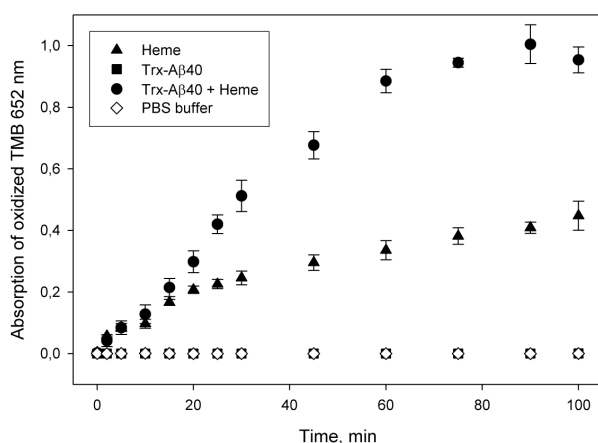


**Fig. 4.** The peroxidase activity of (Trx-A $\beta$ 40)+Heme complex. The oxidation of TMB by (Trx-A $\beta$ 40)+Heme peroxidase was observed by an increase in the absorbance of 652 nm. All tubes contained H<sub>2</sub>O<sub>2</sub>. (Trx-A $\beta$ 40)+Heme was very efficient in oxidation of TMB compared with heme.

### Construction and purification of hybrid A $\beta$ 40 proteins

Genes encoding monomeric and tetrameric streptavidins, hydrophobin, GDH and A $\beta$ 40 were used for the construction of hybrid proteins. The gene constructs *tsa-a $\beta$ 40* and *msa-hfb-a $\beta$ 40* (Fig. 5) were chemically synthesized and cloned into expression vectors pET21d and pET21b, respectively.

**A**



**B**



**Fig. 5.** A) *tsa-a $\beta$ 40* gene construct, which is composed of genes encoding tetrameric streptavidin (*tsa*), polyHis tail, Gly-Ser flexible linker and A $\beta$ 40 peptide. General length of gene construct is 675 bp; B). *msa-hfb-a $\beta$ 40* gene construct, which is composed of genes encoding monomeric streptavidin (*msa*), two Gly-Ser linkers, polyHis tail (*poly-His*), hydrophobin (*hfb*) and A $\beta$ 40 peptide, general length is 933 bp.

The hybrid TSA-A $\beta$ 40 and MSA-HFB-A $\beta$ 40 proteins were expressed when cells were cultivated at 30 °C, induced with 0.5 mM of IPTG at OD<sub>600</sub> 0.8. After induction, cell extracts were analyzed in the 15% SDS-PAGE, where the bands

corresponding the theoretical hybrid protein sizes TSA-A $\beta$ 40 22.72 kDa and 31.86 kDa were observed (Fig. 6). Since the most proteins were insoluble, they were purified under denaturing conditions. Up to 10 mg of pure protein could be obtained from 1 L of culture.

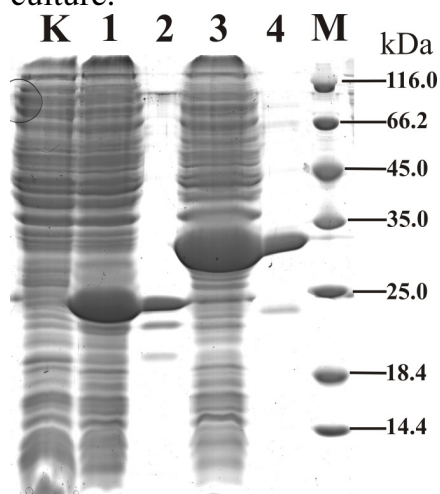


**Fig. 6.** The electrophoretic view of the expression of hybrid proteins in 15% SDS-PAGE. 22.72 kDa band of TSA-A $\beta$ 40 and 31.86 kDa band corresponding MSA-HFB-A $\beta$ 40 were observed. K indicates control – BL21 (DE3) cell extract, 1 – cell extract of TSA-A $\beta$ 40, 2 – purified TSA-A $\beta$ 40, 3 – cell extract of MSA-HFB-A $\beta$ 40 and 4 – purified MSA-HFB-A $\beta$ 40 protein. Mass ruler is marked by M

Genes encoding GDH from *Acinetobacter* sp. and A $\beta$ 40 were fused by cloning *a $\beta$ 40* gene into the plasmid pASKIBA3-PT15 harboring *gdh* gene. Plasmid pPTabpvu16 was obtained, when *a $\beta$ 40* gene was cloned in the middle part of *gdh* gene (this part of gene encodes the loop of protein near the active center of the GDH). Plasmid pPTabeco1 was obtained when *a $\beta$ 40* gene was cloned in the C terminal of *gdh* gene. The hybrid GDH-A $\beta$ 40 proteins were expressed and purified as was described in methods. The expression level of PTabeco1 and PTabpvu16 was lower than wt GDH protein (PT15). The sizes of observed protein bands corresponded to the theoretical sizes (GDH size is 54.2 kDa, GDH-A $\beta$ 40 size is 58 kDa) (Fig.7A).

A $\beta$ 40 was fused to GDH from *E. coli* as well. Gene encoding A $\beta$ 40 peptide was cloned in the plasmid pET-11M-yli1. After transformation and screening two positive clones with plasmids pYliab9 and pYliab10 were obtained. Hybrid proteins were purified under denaturing conditions, since they were expressed in the inclusion bodies. The expression level of hybrid Yliab (GDH-A $\beta$ 40) proteins was significantly higher than wt YliI (GDH) (Fig. 7B); the opposite effect was observed with hybrid PT15 (GDH) and A $\beta$ 40 protein, where the expression of wt PT15 was significantly higher than the expression level of hybrid proteins.

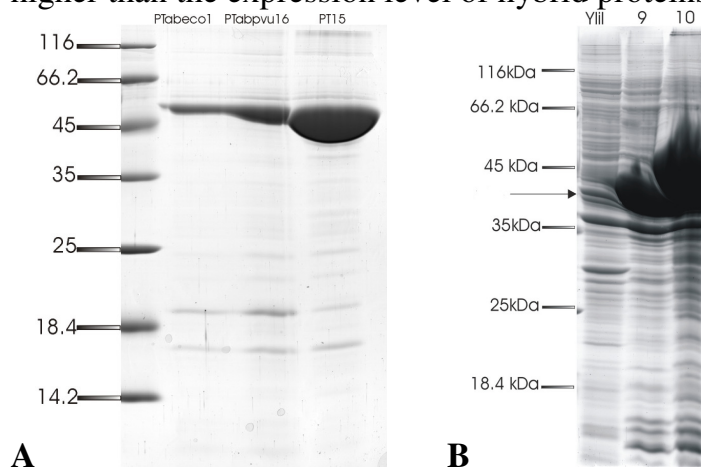


**Fig. 7 A.** The electrophoretic view of purified hybrid A $\beta$ 40 and GDH from *Acinetobacter* sp. proteins (PTabeco1 and PTabpvu16). **Fig. 7B.** The electrophoretic view of expression of hybrid A $\beta$ 40 and GDH from *E. coli*. YliI – GDH, 9 – Yliab9 (GDH-A $\beta$ 40) and 10 – Yliab10 (GDH-A $\beta$ 40).

## Investigation of self-assembling $\beta$ -sheet structures formed by hybrid A $\beta$ 40 proteins

Hybrid TSA-A $\beta$ 40 (SA) and MSA-HFB-A $\beta$ 40 (SHA) proteins also could form fibrillar structures proteins (Fig. 8).

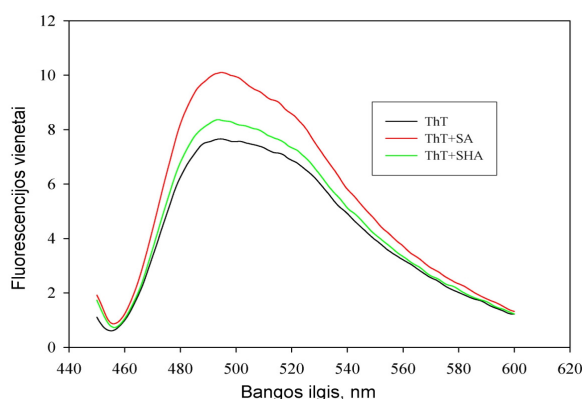


**Fig. 8.** The ThT fluorescence spectra with fibrils of hybrid TSA-A $\beta$ 40 (SA) and MSA-HFB-A $\beta$ 40(SHA) proteins, obtained under acidic conditions (pH 3.0, at 57°C).

ThT fluorescence data showed that hybrid TSA-A $\beta$ 40 (SA) protein formed more fibrils than MSA-HFB-A $\beta$ 40(SHA). The fibrils were visualized with AFM (Fig. 9).

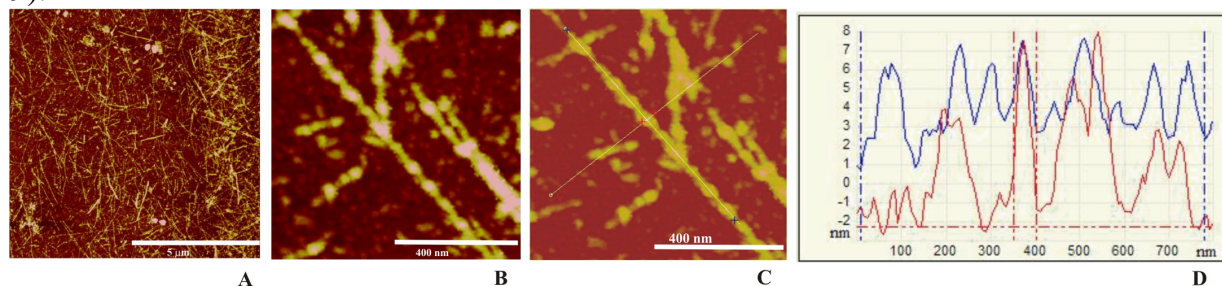


**Fig. 9.** AFM images of TSA-A $\beta$ 40 (SA) protein fibrils. A – Larger scale topography image, B – phase image, C – topography image, and D – cross-section profiles of fibrils. The scale and profiles are marked with white bars.

It was determined that SA protein formed heteromorphous twisted fibrils with medium height of 5.5 nm, when fibrillization was performed at pH 3.0 (Fig. 9). Comparing the fibrils which were formed by A $\beta$ 40 peptide and hybrid SA protein it turned out that the height is similar, but hybrid protein formed more structured fibrils.

AFM images of SHA fibrils confirmed the result from the measurements with ThT. SHA hybrid protein was able to form fibrils, but less than SA protein. This protein was prone to form amorphous aggregates and it was very unstable in the solution. It might be that hydrophobin influenced the solubility of the whole hybrid protein. However the height of fibrils remains similar to SA protein formed fibrils (~5 nm) (Fig. 10).

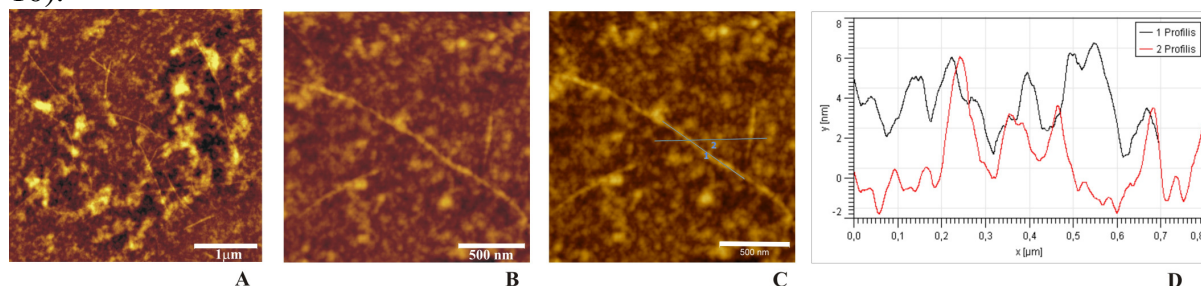


**Fig 10.** AFM images of MSA-HFB-A $\beta$ 40 (SHA) protein fibrils. A and B demonstrate topography images, C and D cross-section profiles. The scale and profiles are marked with white bars.

SDS-PAGE analysis proved that fibrils of hybrid SA and SHA proteins, obtained at pH 3.0, degraded into smaller fragments.

Since the aim was to construct functional fibrils, the ones that were obtained at pH 3.0 were not suitable, since streptavidin was not intact. Hence, the fibrillization conditions were altered, and protein was fibrillized under milder acidic conditions (10 mM Na-acetic buffer, pH 4.6). In this case, SA protein formed fibrils and remained stable. The activity of tetrameric streptavidin was demonstrated with biotin conjugated with stilbazole fluorophore. It was supposed, that if tetrameric streptavidin take its active conformation, it may form a net-like structure. To confirm the hypothetical model, AFM images were obtained and net-like structure was observed (Fig. 11). The height of fibrils that formed the net was 2.5–4.5 nm.

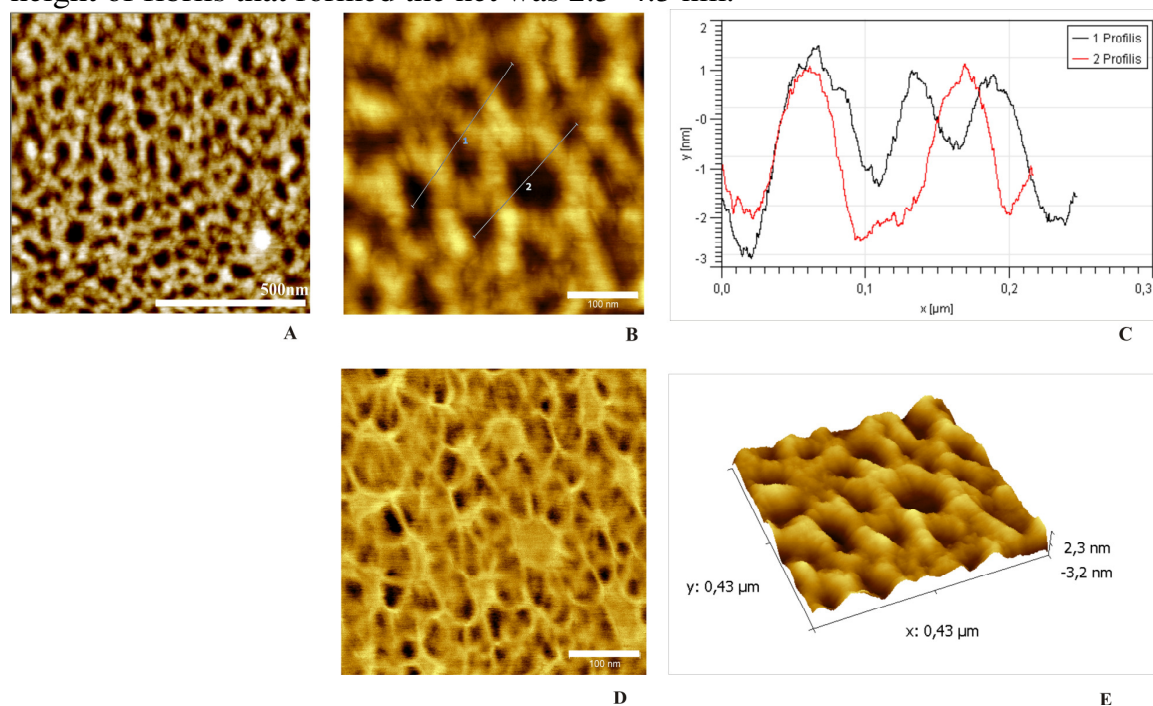


**Fig. 11.** AFM images of fibrils formed by hybrid streptavidin-A $\beta$ 40 (SA) protein. A – General topography view, B and C – cross-section profiles, D – phase view, E – 3D view of fibrillar structure. The scale and profiles are marked with white bars.

Constructed hybrid A $\beta$ 40 and GDH proteins were less prone to self-aggregate under conditions that are relevant to the GDH activity. A $\beta$ 40 peptide was used as a seed for the fibrillization of hybrid GDH-A $\beta$ 40 (PTabeco1) protein. The following samples were prepared: A $\beta$ 40 peptide 2 mg/ml (F1), A $\beta$ 40 peptide 2mg/ml with PTabeco1 1 mg/ml (F2), PTabeco1 1 mg/ml (F3), PTabeco1 5 mg/ml (F4), PTabeco1 5 mg/ml, pH 2 (F5). The samples of fibrils were evaluated by measuring the increase of ThT fluorescence (Fig. 12).

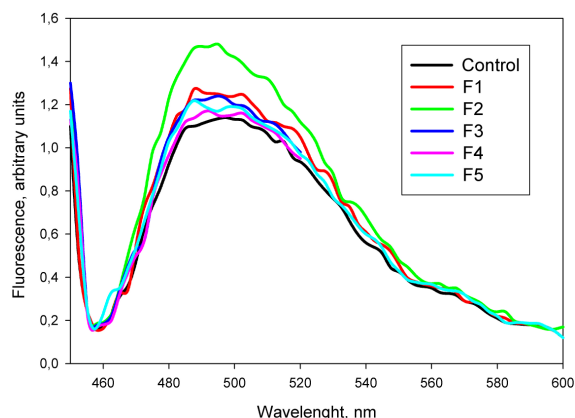


**Fig. 12.** ThT fluorescence spectra with hybrid GDH and A $\beta$ 40 protein fibril samples. F1 – A $\beta$ 40 peptide 2 mg/ml (pH 7.0), F2 – A $\beta$ 40 2 mg/ml with PTabeco1 1 mg/ml (pH 7.0), F3 – PTabeco1 1 mg/ml (pH 7.0), F4 – PTabeco1 5 mg/ml (pH 7.0), F5 – PTabeco1 5 mg/ml (pH 2.0), Control – ThT solution without proteins.

The most intensive fluorescence was observed in the case of F2 sample in which A $\beta$ 40 peptide and hybrid GDH-A $\beta$ 40 (PTabeco1) was fibrillized. Weak interactions of other samples with ThT showed that there were less fibrillar aggregates. Therefore, the samples were incubated for a few months at 4 °C and then analyzed with AFM tapping mode. The AFM images showed that hybrid GDH-A $\beta$ 40 (PTabeco1) and hybrid GDH-A $\beta$ 40 (PTabpvu16) formed fibrils of distinct morphology (Fig. 13).

When hybrid GDH-A $\beta$ 40 (PTabeco1) protein was fibrillized with A $\beta$ 40 peptide, structurized fibrils were observed, in contrast to A $\beta$ 40 fibrils that are straight and unbranched. The fibrils obtained from hybrid proteins were thicker and shorter and formed ringed shape structures with the height of 3.5–5.0 nm (Fig.13). When GDH-A $\beta$ 40 (PTabeco1) was fibrillized under the same conditions but without seeding with A $\beta$ 40, thin broken ringed shape fibrils were observed (Fig. 13). The height of fibrillar structures was ~ 5.0 nm. Nevertheless, SDS-PAGE analysis showed that nearly all of proteins degraded into smaller fragments, which were larger than A $\beta$ 40, hence we assumed that the fibrils were composed of A $\beta$ 40 and GDH fragments. Hybrid GDH-A $\beta$ 40 (PTabpvu16) protein was incubated at 4 °C for 6 months and formed fibrils of distinct morphology than the fibrils formed by GDH-A $\beta$ 40 (PTabpvu16) (Fig. 13). GDH-A $\beta$ 40 (PTabpvu16) formed twisted rope like structures with the height of 5–7 nm. SDS-PAGE analysis showed that this hybrid protein degraded into smaller fragments. Interestingly, the hybrid GDH-A $\beta$ 40 (YliabI) protein did not form fibrils under acidic or neutral conditions.

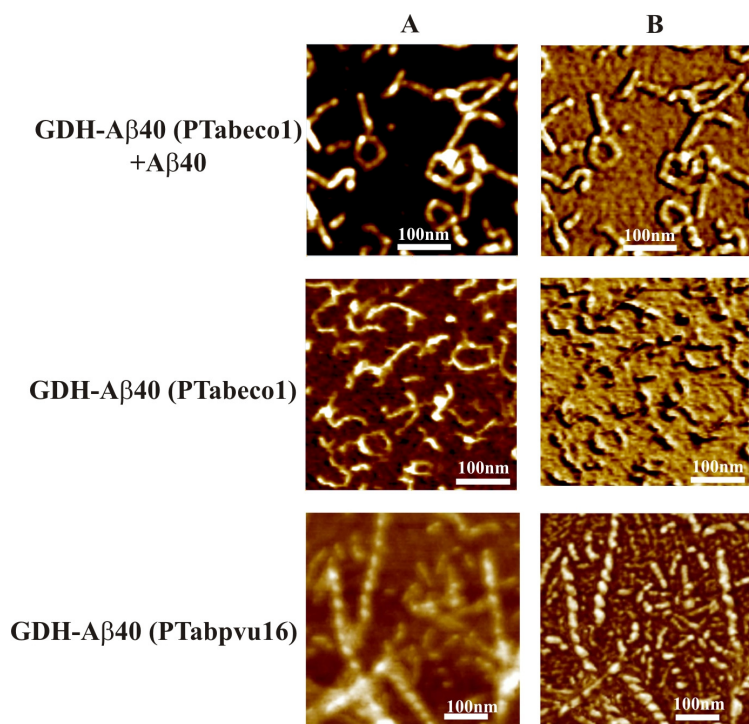


**Fig. 13.** The AFM images of hybrid GDH-A $\beta$ 40 (PTabeco1) and GDH-A $\beta$ 40 (PTabpvu16) fibrils. A – Topography image, B – Phase image. GDH-A $\beta$ 40+A $\beta$ 40 – samples, where A $\beta$ 40 peptide was used as seed. The scale is marked with white bar.

### The modification of mutant A $\beta$ 40cys2 and A $\beta$ 40cys39 peptides

It was determined that A $\beta$ 40cys2 and A $\beta$ 40cys39 peptides formed fibrillar structures. These peptides were modified by 5 nm gold nanoparticles which were added before and after the fibrillization.

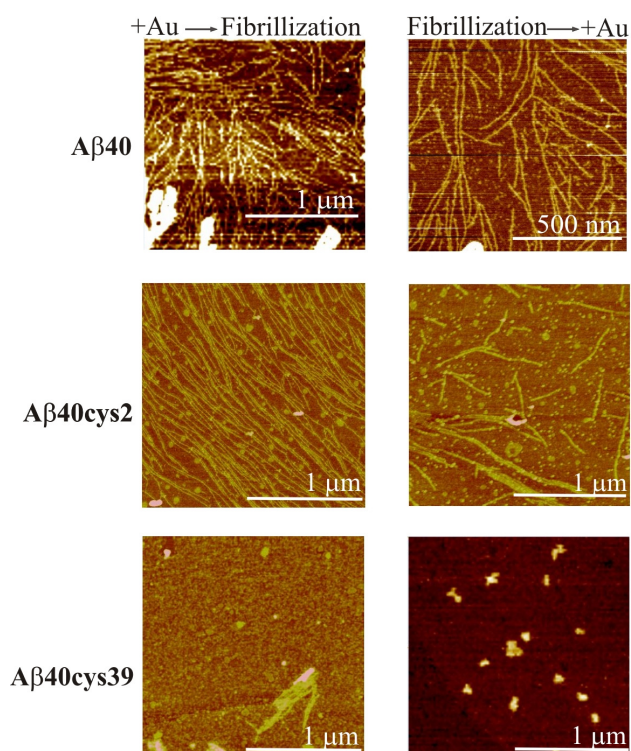


**Fig. 14.** The influence of gold nanoparticles to the aggregation of A $\beta$ 40 and its mutants (A $\beta$ 40cys2 and A $\beta$ 40cys39).

The samples were analyzed by measuring ThT fluorescence, and the results of spectra showed that gold nanoparticles positively influenced the formation of fibrils. In the case of A $\beta$ 40 and A $\beta$ 40cys2, more fibrils were formed when peptides were fibrillized with gold nanoparticles. A $\beta$ 40cys39 formed less fibrillar structures and gold

nanoparticles did not have an impact. The same samples were analyzed by AFM tapping mode (Fig. 14) which confirmed the results obtained from the measurements with ThT.

## THE INVESTIGATION OF AGGREGATION OF $\alpha$ -SYNUCLEIN ( $\alpha$ -SYN) DERIVATIVES

$\alpha$ -Syn is a small protein that is known to form fibrils and thus it can be applied in the nanoconstruction.

### The construction and purification of $\alpha$ -Syn derivatives

$\alpha$ -Syn<sub>cys141</sub> mutant that had an additional amino acid – cysteine at the 141 position was constructed. The best expression was observed when cells were cultivated at 37 °C until OD<sub>600</sub> reached 0.8 and induced with 0.2 mM IPTG, and continued cultivating for 4 h at 30 °C.  $\alpha$ -Syn and  $\alpha$ -Syn<sub>cys141</sub> were soluble after heating, but many proteins denatured and were separated by centrifugation. After the first purification, proteins were not pure; therefore, the second purification step was required. About 18 kDa bands were observed after SDS-PAGE analysis (Fig. 15). However, theoretical molecular mass of  $\alpha$ -Syn is 14.46 kDa, but it was assumed that very acidic C terminal of  $\alpha$ -Syn weakly interacted with SDS and therefore it migrated as a 18 kDa (Giehm et al., 2011). About 15 mg of both proteins could be obtained from one liter of culture

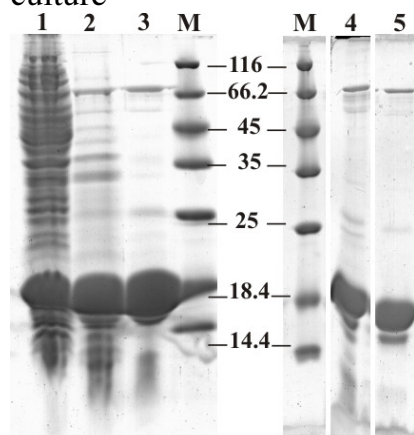


**Fig. 15.** The electrophoretic view of  $\alpha$ -Syn<sub>cys141</sub> purification steps. 1 – protein extract; 2 –  $\alpha$ -Syn<sub>cys141</sub> protein extract after heating at 100 °C; 3 and 4 – protein after purification with Q XL column, 5 – protein after additional purification with ANX column. M indicates the molecular mass ruler.

Hybrid protein was constructed using genes encoding  $\alpha$ -Syn and dimeric GDH from *Acinetobacter* sp.  $\alpha$ -Syn gene was inserted in the C terminal region of GDH gene in plasmid pASKIBA3-pT15. Hybrid (PTsyneco) protein was expressed and purified as described in methods.

### Investigation of self-assembling $\beta$ -sheet structures formed by $\alpha$ -Syn derivatives

$\alpha$ -Syn<sub>cys141</sub> formed fibrils distinct to  $\alpha$ -Syn formed structures. At the acidic pH (pH 2.7) both proteins produced the fibrillar structures, but after SDS-PAGE analysis it turned out, that proteins degraded into smaller fragments able to form fibrils (Fig. 16).

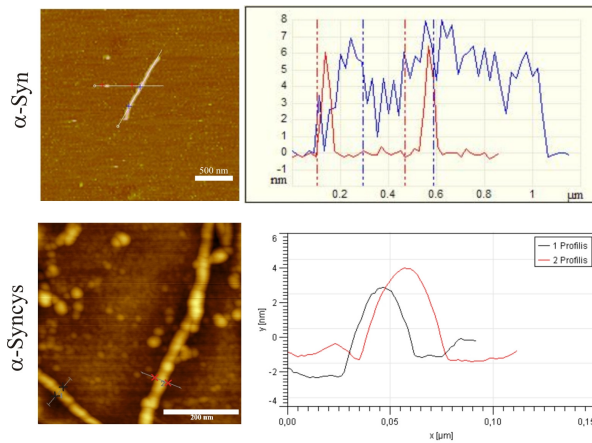


**Fig. 16.**  $\alpha$ -Syn and  $\alpha$ -Syncys141 fibrils and their profiles obtained under acidic conditions (pH 2.7) by AFM.

The fibrils of different morphology were observed in AFM images.  $\alpha$ -Syn formed long unbranched structures which were 5.0–8.0 nm in height, while  $\alpha$ -Syncys141 fibrils were long segmented and were 4.5–7.0 nm in height. When  $\alpha$ -Syncys141 and  $\alpha$ -Syn proteins were fibrillized at pH 7.5 (Luk et al., 2009) different fibrils were observed and proteins remained intact.  $\alpha$ -Syn protein formed fibrils of average 4.5 nm height and  $\alpha$ -Syncys141 fibrils were thinner than  $\alpha$ -Syn fibrils and were of average 3.5 nm in height (Fig. 17).

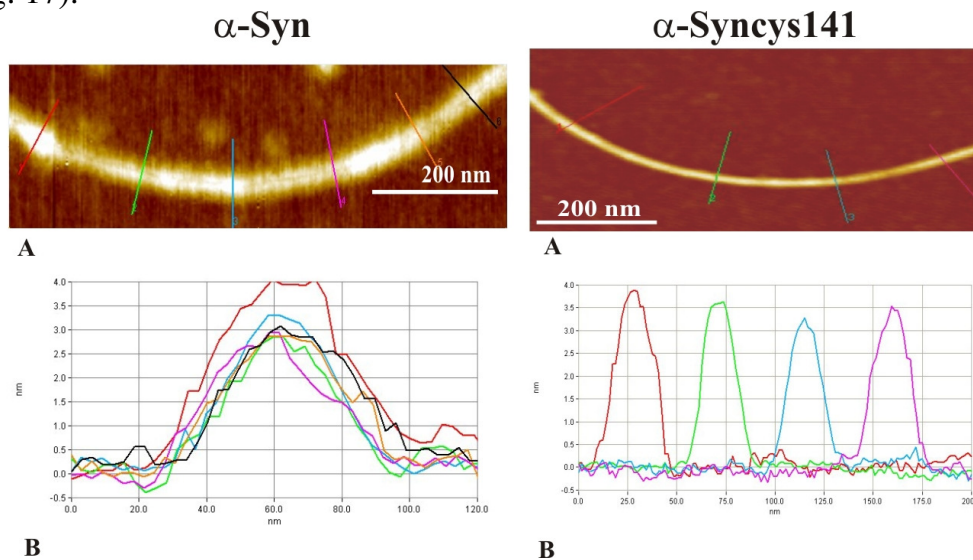


**Fig. 17.**  $\alpha$ -Syn and  $\alpha$ -Syncys141 fibrils obtained at pH 7.5. A – topography view, B – cross-section profiles.

The fibrils formed by  $\alpha$ -Syn and  $\alpha$ -Syncys141 were evaluated by ThT fluorescence.  $\alpha$ -Syncys141 protein formed more fibrils than  $\alpha$ -Syn.

Hybrid GDH and  $\alpha$ -Syn proteins were fibrillized at 37 °C, different pH (from 2.5 to 9.5). In some samples additional  $\alpha$ -Syn was added (Fig. 18). After fibrillization, proteins were analyzed in SDS-PAGE. Under acidic conditions, the bands corresponding the size of hybrid PTsyneco protein disappeared. Since new bands appeared, it can be concluded, that PTsyneco self-assembled into higher structures (oligomers and fibrils). The formation of fibrils was verified with interaction with ThT



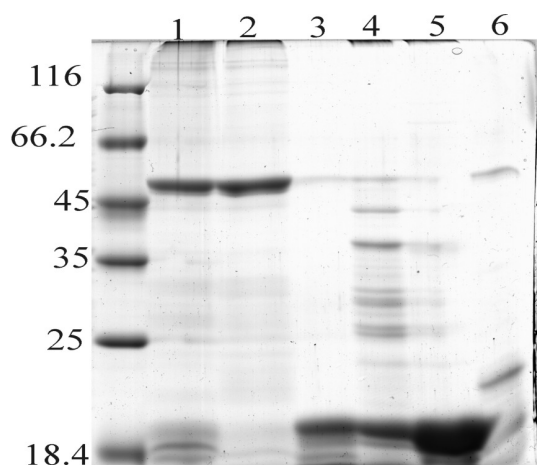


**Fig. 18.** The electrophoretic view after two-week fibrillization at 37 °C. 1.  $\alpha$ -Syn + PTsyneco (pH 9,5), 2.  $\alpha$ -Syn + PTsyneco (pH 7,5), 3.  $\alpha$ -Syn+PTsyneco (pH 4,6), 4.  $\alpha$ -Syn + PTsyneco (pH 2,7), 5.  $\alpha$ -Syn (pH 7,5), 6. PTsyneco (pH 7,5).

Most fibrils formed when PTsyneco was fibrillized with  $\alpha$ -Syn (4 mg/ml: 0.8 mg/ml) at pH 2.7 for two weeks at 57 °C. After fibrillization  $\alpha$ -Syn protein formed fibrils of about ~ 3.0 nm in height, the hybrid PTsyneco protein also formed structures of ~3.0 nm in height. When PTsyneco protein was fibrillized in the presence of  $\alpha$ -Syn, uneven fibrils were observed. It was concluded that these hybrid fibrils were formed from PTsyneco and  $\alpha$ -Syn (Fig. 19).

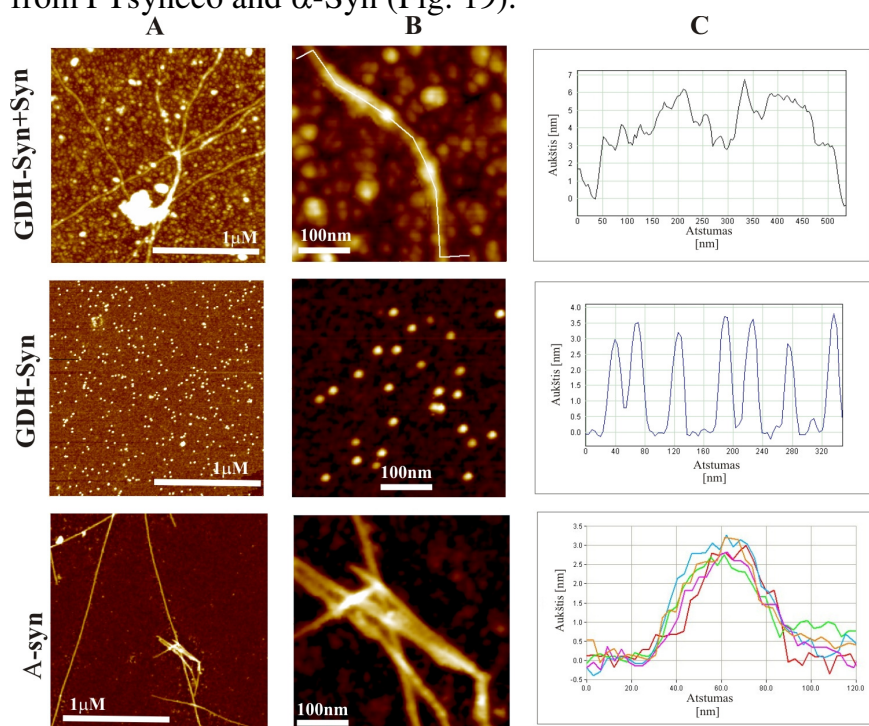


**Fig. 19.** The AFM images of hybrid PTsyneco protein and  $\alpha$ -Syn fibrils. A and B – topography images, C – cross-section profiles

Although hybrid PTsyneco protein degraded, fibrillar structures that differed from  $\alpha$ -Syn fibrils, were observed.  $\alpha$ -Syn formed fibrils of 3–3.5 nm in height. Hybrid PTsyneco protein formed homogeneous non-filamentous structures of 3.5 nm in height. When  $\alpha$ -Syn was fibrillized in the presence of PTsyneco, heteromorphic fibrils were observed whose height reached 3.5 nm (same as  $\alpha$ -Syn fibrils) and 6.5 nm.

### The modification of fibrils formed by $\alpha$ -Syn<sub>141</sub>

Prior to the biotinylation of fibrils, TCEP was added to obtain free thiol groups as disulfide bonds could be formed when two  $\alpha$ -Syn<sub>141</sub> proteins interact. The reduction with TCEP did not disarrange the fibrillar structures. Biotinylated  $\alpha$ -Syn<sub>141</sub> proteins were dialyzed and gold nanoparticles conjugated with neutravidin

molecules were attached. 10 nm gold nanoparticles had two neutravidin molecules that could couple two fibrils by binding to biotins (Fig. 20).

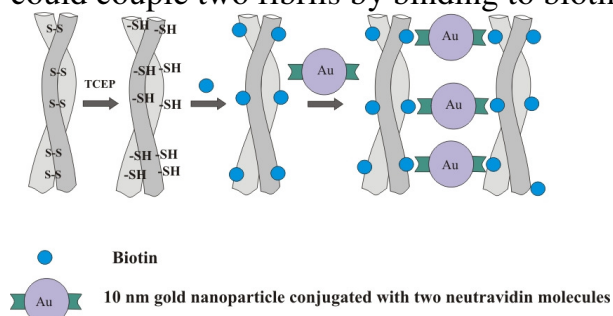


**Fig. 20.** Hypothetical scheme of the formation of  $\alpha$ -Syncys141 fibrillar structures modified with conjugated with neutravidin molecules gold nanoparticles. Two biotinylated fibrils coupled with the gold nanoparticle conjugated with neutravidin

After modification,  $\alpha$ -Syncys141 fibrils were evaluated by AFM (Fig. 21) and electron transmission microscope (TEM) (Fig. 22).

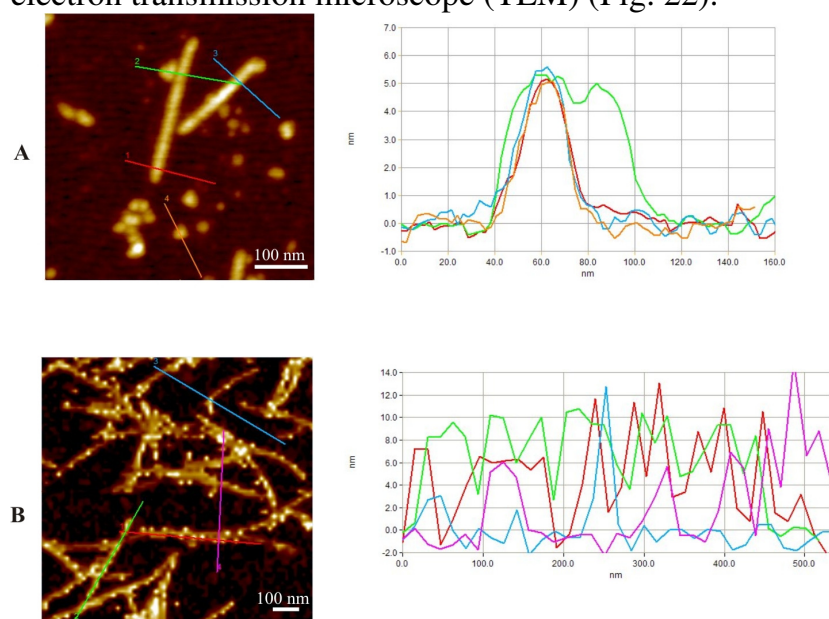


**Fig. 21.** AFM topography images and cross-section profiles of  $\alpha$ -Syncys141 fibrils modified with biotin (A) and modified with biotin and gold nanoparticles conjugated with neutravidin molecules (B).

After modification with biotin, the height of fibrils was about 5 nm. The height of gold nanoparticles is 10 nm. Fibrils with higher structures attached were observed in AFM images. The cross-section profiles showed that about 10 nm high structures were attached to biotinylated  $\alpha$ -Syncys141 fibrils. Therefore, it was assumed that biotinylated  $\alpha$ -Syncys141 fibrils were successfully modified with gold nanoparticles conjugated with neutravidins. TEM images verified the results obtained from AFM images.

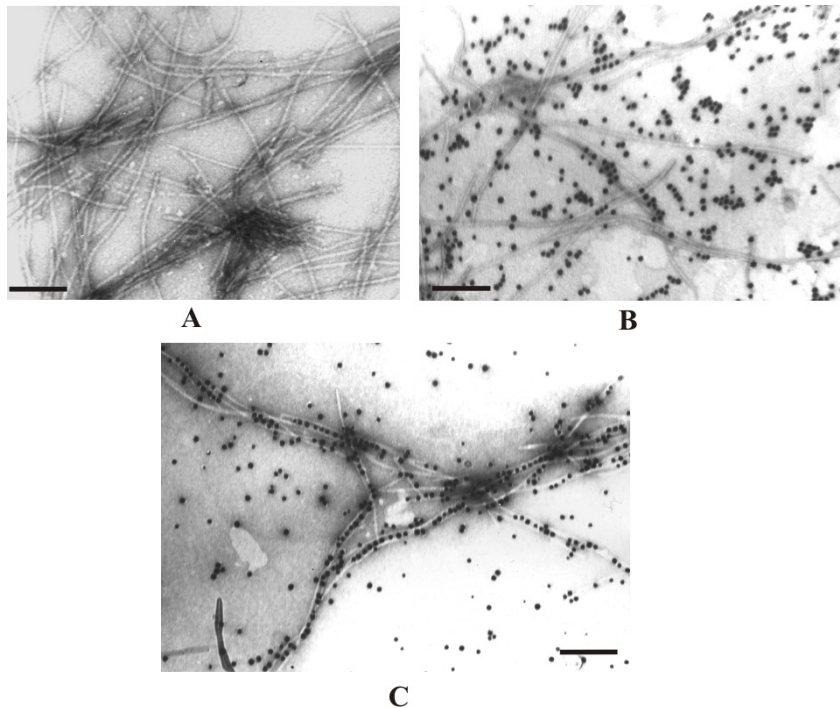


**Fig. 22.** TEM image of modified  $\alpha$ -Syncys141 fibrils. A.  $\alpha$ -Syncys141 fibrils, B.  $\alpha$ -Syncys141 fibrils modified with biotin and gold nanoparticles conjugated with neutravidins. C.  $\alpha$ -Syncys141 fibrils modified with biotin and gold nanoparticles conjugated with neutravidins after a week. Bar indicates 100 nm. Magnification is 100000 times.

After modification with gold nanoparticles,  $\alpha$ -Syncys141 fibrils assembled into the hybrid ladder-like nanostructures. The level of assemblage was time dependent. These ladder nanostructures (Fig. 23) confirmed the theoretical scheme of formation of hybrid nanostructures (Fig. 20).

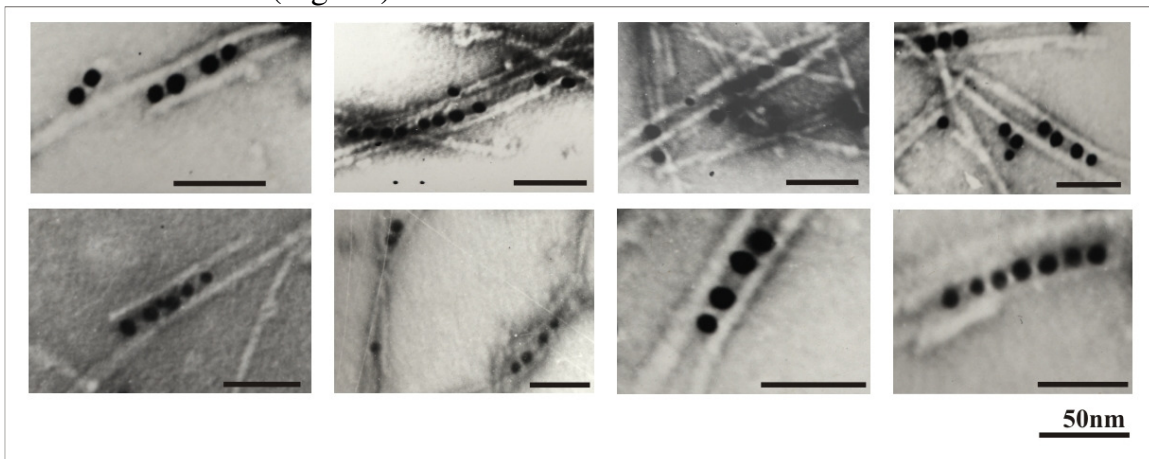


**Fig. 23.** The TEM images of the ladder-like nanostructures composed of two biotinylated  $\alpha$ -Syncys141 fibrils coupled with conjugated gold nanoparticles.

## INVESTIGATION OF EQUINE LYSOZYME (EL)

### Construction and purification of EL in *E. coli* cells

Different fusion agents were used for the purification of EL. Though only two constructs pM50-EL4 (harbouring DsbA fused to EL in pETM-50 vector) and pM11EL13 (encoding the EL with N-terminal His tag in pETM-11 vector) produced hybrid proteins visible in PAGE. The hybrid protein M50-EL4 was probably transferred into the periplasmic space of *E. coli* strain C43 (DE3). Since the fused protein was active, the host cells were lysed during the induction step, making the growth of cells hard to control. The pM11EL13 construct produced  $\sim 50$  mg of protein from 1 L of culture when expressed in the *E. coli* strain BL21 (DE3) and 20 mg/L in the *E. coli* strain C43 (DE3), but the recombinant protein was expressed as the inclusion bodies. Addition

of  $\text{CaCl}_2$  to the medium did not influence the expression, solubility or stability of the M11EL13 protein. The protein expressed as inclusion bodies was solubilized in 6 M urea and purified by Ni-chelating column. Denatured recombinant lysozyme was refolded by dialysis against buffer containing  $\beta$ -ME and 10 mM arginine (Bajorunaite et al., 2007). About 80% of the protein was soluble after refolding and the His tag was removed by proteolysis with TEV protease. Three additional amino acid residues (Gly-Ala-Met) were remaining at the recombinant protein (EL13) N-terminus compared with the native protein. An additional purification step using SP-Sepharose ion exchange chromatography was introduced to remove TEV protease. Both EL13 and TEV were adsorbed onto the SP column. TEV was removed from the column in the presence of 100 mM NaCl and EL13 was eluted at 250 mM of NaCl (Fig. 24). The recombinant His-tagged protein (M11EL13) showed a very low activity and the specific activity was not higher than  $5 \pm 1$  U/mg protein. The specific activity of the recombinant EL (EL13), after removing the tag, increased up to  $25\,000 \pm 3000$  U/mg.

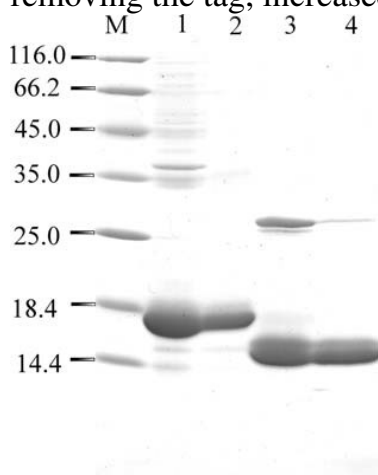


**Fig. 24.** Purification of the recombinant EL. Lane 1: solubilized inclusion bodies from *E. coli* BL21 (DE3) (pM11EL13); lane 2: His-tagged hybrid protein M11EL13 eluted from Ni-chelating column; lane 3: hybrid protein M11EL13 after incubation with TEV protease; lane 4: EL13 lysozyme after elution from Sepharose SP FF column. M, molecular mass marker (kDa).

### Investigation of aggregation of EL

EL was fibrillized as described in methods. Since the native EL formed ring-shaped and filamentous structures in the solution at pH 4.5 and 55–57 °C (Malisauskas et al., 2003), the similar conditions were chosen for the fibrillization of the recombinant EL. About 1 and 10 mg/ml were incubated for 5–6 days at 55 °C, with or without  $\text{CaCl}_2$ . After 1 day of incubation gel-like structure was observed in the 10 mg/ml samples. ThT bound to the formed fibrils as seen from the increased fluorescence of dye (Fig. 25).

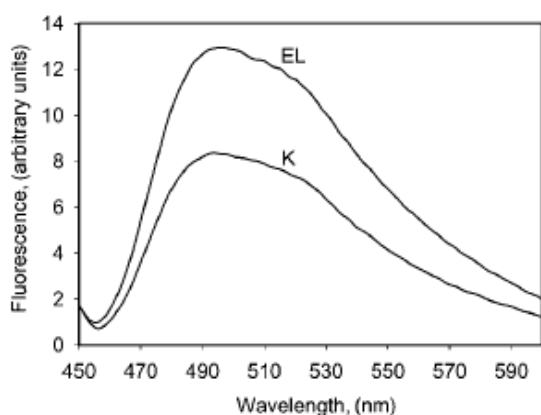


**Fig. 25.** Changes in the fluorescence spectra of ThT in the presence of EL. ThT (10 mM final concentration) was incubated with 0.01% of protein for 3 min before measurement. Emission spectra of ThT were recorded (excitation at 450 nm) in the presence (EL) and absence (K) of lysozyme.

AFM revealed several types of fibril structures among which the closed rings and the bent or straight short aggregates were observed (Fig. 26). EL13 in the presence of 10 mM CaCl<sub>2</sub> formed circular amyloid structures and linear bent aggregates. The linear structures were ca. 100–300 nm in length and ca. 3 nm in height. Cross section of the filament along its axis demonstrated that it is a segmental structure, with height variation from 1.5 to 3.0 nm (Fig. 26A). This observation indicates that filaments were divided into segments. Ring-shaped structures are ca. 80 nm in diameter and ca. 3 nm in height (Fig. 26 B and C). In the absence of CaCl<sub>2</sub>, the same structures were observed. The dominant form of fibrils in both protein samples was ring shaped.

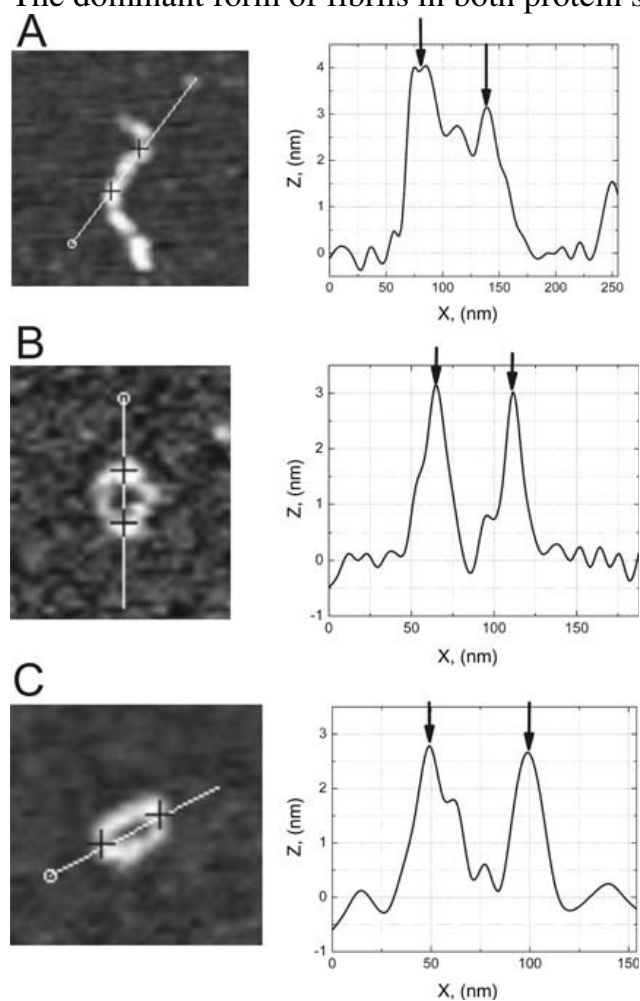


**Fig. 26.** AFM images of the structures of recombinant EL at pH 4.5 and 55 °C. A direction of the cross sections of the structures is shown on the left. Cross-marked points on the left side correspond to arrows on the right side of images where the height profiles are presented. (A) The fibril-like structure. (B) The ring-shaped structure. (C) The ellipse-like structure.

The stability of the recombinant EL13 was also very similar to that of the native EL. After 7 days of incubation at 55 °C and pH 4.5, the EL13 degraded. Similar results were obtained for the native EL. The protein was fragmented under acidic conditions (pH 2.0) during the prolonged incubation (after 2 days at 57 °C and after 8 days at 37 °C). Although after 7 days of incubation at pH 4.5 and 57 °C only 14,645 Da protein corresponding the intact EL was observed (Malisauskas et al., 2003).

## Discussion

Biomolecules are especially attractive building blocks for molecular self-assembly. A $\beta$ 40 peptide was used to construct mutant and hybrid proteins. The formation of fibrillar structures of A $\beta$ 40 derivatives was investigated under various fibrillization conditions. The expression and purification system was applied for the

preparation of the recombinant peptide, which was used for the further experiments. Thioredoxin, which is very frequently used as a fusion partner (Thapa et al, 2008) was applied in the purification of A $\beta$ 40 peptide. A $\beta$  peptides are too small and toxic to be cultivated in bacteria. Therefore, the fusion agents that facilitate the purification of A $\beta$  peptides are often used (Hammarström et al., 2002; Wiesehan et al, 2007; Walsh et al, 2009; Zhang et al, 2009).

The fused Trx-A $\beta$ 40 protein was used to determine whether His residues in A $\beta$ 40 sequence had been responsible for heme binding. The results showed that histidine residues in A $\beta$ 40 peptide sequence had been participating in heme binding. It turned out that the binding efficiency decreased when histidine codons were altered, while the interaction between Trx-A $\beta$ 40 and heme was very strong. This showed that A $\beta$ 40 is responsible for the interaction of Trx-A $\beta$ 40 with heme. Heme was shown to inhibit *in vitro* aggregation of A $\beta$ 40 and A $\beta$ 42 (Howlett et al, 1997). Nevertheless, His was known to bind with heme in several heme proteins. Additionally, A $\beta$ 40 contained hydrophobic amino acids (two Leu residues and three Ile residues) and the amino acids Asn and Gln, which are usually found in heme-binding pockets of heme proteins (Atamna and Boyle, 2006). Furthermore, an increase in absorbance was observed at 530–550 nm only in the case of Trx-A $\beta$ 40. Atamna and Boyle also observed such an increase in this range with A $\beta$ 42. This can be explained by some redox reactions between iron ion of heme and A $\beta$ 40, but more experiments are necessary to elucidate the origin of increase at 530–550 nm. Moreover, the complex of hybrid protein Trx-A $\beta$ 40 and heme showed peroxidase activity. The amino acid sequence of A $\beta$ 40 contained Arg, His and Phe, which participated in the H<sub>2</sub>O<sub>2</sub> binding and catalyzed the heterolytic split of O–O bond of H<sub>2</sub>O<sub>2</sub> of peroxidases (Fukuyama et al., 1995). Still, more experiments are necessary to explain the full mechanism of heme binding.

The AFM images showed that A $\beta$ 40 fibrils are very polymorphic. A $\beta$ 40 and its mutant variants A $\beta$ 40cys2 and A $\beta$ 40cys39 formed similar fibrils, assuming that the morphology of fibrils differed according to the preparation. A $\beta$ 40 peptide formed more fibrillar structures than A $\beta$ 40cys2 and A $\beta$ 40cys39. It was known that the C terminal of A $\beta$ 40 in water was unstructured (Sgourakis et al., 2007). It might be that alteration of Val in the 39 position to Cys is an obstacle, to oligomerize into larger fibrillar structures, occurred. A $\beta$ 40 fibrils characterized in the literature were 3.5–13 nm in height, the length reached several microns, and fibrils were long and unbranched. The fibrils, obtained in this work, formed similar fibrils as were described in literature. It was determined that gold nanoparticles positively influenced the aggregation of peptides. After the experiment it turned out, that A $\beta$ 40cys2 peptide can be applied in the nanoconstruction.

The hybrids formed of A $\beta$ 40 and different proteins were constructed to find out whether they could be applied in the design of nanostructures, where A $\beta$ 40 would form nanotemplate and proteins would fulfill their function (GDH and streptavidin). Constructed hybrid GDH-A $\beta$ 40 proteins self-arranged into fibrils after long incubation, but the activity of GDH was not detected. Caine et al. data demonstrated that GFP-A $\beta$ 42 fusion protein was constructed, but when fibrils were formed, the activity of GFP was inhibited (Caine et al., 2007). More experiments are required to elucidate the optimal conditions to keep GDH active.

The hybrids constructed from streptavidin and A $\beta$ 40 formed fibrils under appropriate conditions as well. It was determined that this hybrid protein formed a net-like structure, which could be used as immobilizing template, when pH was 4.6. There are reports about fibrillar matrixes, where enzymes were immobilized. For instance, the immobilization of glucose oxidase (GOD) onto nanoscaffolds formed by amyloid fibrils from bovine insulin using glutaraldehyde. Such functionallization was successful, because GOD kept its activity. Immobilized GOD was introduced into PVOH films; therefore, a novel bionanomaterial was obtained (Pilkington et al., 2009). Although GOD is more frequently used in the glucose industrial measurements (Yoshida et al., 2003), PQQ-GDH is used in the production of biosensors (Tanaka et al., 2005; Hamamatsu et al., 2006).

The aggregation of the 140 aa protein  $\alpha$ -Syn is associated with a prominent cytopathological hallmarks of Parkinson's disease. The results of the experiments proved that  $\alpha$ -Syn protein was convenient protein to use it for nanobiotechnological applications. Firstly, the purification of this protein is very simple and effective procedure, secondly, relatively high yield of this protein can be obtained. Therefore,  $\alpha$ -Syn<sub>Cys141</sub> mutant, which was easy to handle either, was constructed. The yield and the purity were similar to  $\alpha$ -Syn protein. There are reports about the utilization of  $\alpha$ -Syn protein in the construction of nanoobjects. Yuschenko et al. constructed AS140-MFC that was the Cys mutant of  $\alpha$ -Syn in position 140 (C-terminus) reacted with a thiol-reactive maleimide probe (MFC) based on 2-(2-furyl)-3-hydroxychromone FC. Labeled AS140-MFC construct was fibrillized and according to the fluorescence intensity the level of fibrillization was measured (Yuschenko et al., 2010).  $\alpha$ -Syn (E46K) mutant protein was used as template for construction of palladium, copper, and gold nanowires (Colby et al., 2008). All the experiments with  $\alpha$ -Syn modification that had been reported are based on the protein but not fibril modification. In this work, it was demonstrated that  $\alpha$ -Syn<sub>Cys141</sub> protein with introduced additional amino acid – cysteine in the 141 position formed filamentous fibrils similar to fibrils formed by  $\alpha$ -Syn. The fibrillar aggregates could be modified with biotin and then assembled with gold nanoparticles conjugated with neutravidin molecules.  $\alpha$ -Syn<sub>Cys141</sub> protein was an excellent building block in the construction of nanoobjects.

The possibilities to use recombinant amyloid equine lysozyme (EL) in the fibrillization were also investigated. The aim of this study was to create an expression system of EL in *E. coli*. Previously the recombinant EL was only expressed in the filamentous fungi (Spencer et al., 1999). The disadvantages of this expression system were posttranslational modifications existing in *A. niger*, acidic conditions during the growth of the organism, which destabilized the EL and a difficult purification procedure (Spencer et al., 1999). Purification from the mare milk was not complicated (Noppe et al., 1996), but for some investigation, a recombinant protein is required. Among the recombinant lysozymes only a few of them were soluble when expressed in *E. coli*: the human lysozyme in the presence of the trigger factor and GroEL-GroES chaperones (Nishihara et al., 2000), the hen-egg lysozyme expressed as the OmpA-fused soluble protein (Fischer et al., 1993) and the lysozyme from *Hirudo medicinalis* (Zavalova et al., 2004). In all cases when lysozyme was expressed as a soluble protein this led to the breakdown of the cells (hen-egg (Fischer et al., 1993) and medicinal leech lysozymes (Zavalova et al., 2004)) or the specific activity was much lower than the specific activity

of the authentic protein [human lysozyme (Nishihara et al., 2000)]. The His-tagged EL was expressed in the form of inclusion bodies. Such behaviour was also observed in the case of other lysozymes. These include canine (Koshiba et al., 1999), hen-egg (Schlorb et al., 2005) and *Tapes japonica* (Takeshita et al., 2004) lysozymes. However, the expression level differed: 50 mg/l of culture for the canine lysozyme, 25 mg/l in the case of hen-egg lysozyme, 10 mg/l for *T. japonica* and 0.6 mg/l for tobacco hornworm (*Manduca sexta*) (Garcia-Orozco et al., 2005). The expression level of EL reached during this study (50 mg/l of culture) was most similar to the canine lysozyme. The refolding procedure was a critical step in the purification of the EL. Arginine was found to be applicable for the refolding of EL; however, a part of the EL (about 20%) precipitated due to misfolding. After solubilization, refolding and proteolysis, a pure recombinant EL was active. The specific activity (25 000 U/ mg) was lower than the native (38 000 U/mg) or *A. niger* (37 500 U/mg) produced ELs (Spencer et al., 1999). A possible explanation for this difference is that the recombinant EL (variant EL13) expressed in *E. coli* possessed three additional N-terminal amino acid residues (glycine, alanine and methionine), required for the construction of the recombinant plasmid and protease digestion. These additional amino acid residues could influence protein properties and folding; as it is known that even one additional methionine residue at N-terminus affected the stability and solubility of  $\alpha$ -lactalbumin and lysozymes when these proteins were expressed in *E. coli* (Takano et al., 1999; Mine et al., 1997; Ishikawa et al., 1998). The His-tagged EL was almost inactive prior to TEV proteolysis. Its activity was about 5000 times lower than those of the EL13 after the protease digestion. Hence, alterations of the protein N-terminus were responsible for the EL activity. Despite the incorrect folding during the growth, recombinant EL13 took the correct active structure after refolding and proteolysis. Moreover, it formed amyloidal structures, analogical to the native protein under the destabilizing conditions. The  $\text{Ca}^{2+}$  influence on the fibril formation of the recombinant EL was different from those of the native protein. For the recombinant EL, ring forms and straight fibrils were observed both in the presence and absence of  $\text{Ca}^{2+}$ , the dominant form in both cases were ring-shaped structures. The native EL predominantly formed the ring-shaped fibrils in the absence and the straight fibrils in the presence of  $\text{Ca}^{2+}$  (Malisauskas et al., 2003). It is interesting to note that under fibrillization conditions, the same as for the recombinant EL, the protein with the His-tag did not form any filamentous structures. Only amorphous aggregates were produced under these conditions (data are not shown). The His-tag hindered not only the formation of active protein but also the formation of the fibril structures. The expression of EL in *E. coli* reached a high level and may be further enhanced by optimizing the culture conditions and adjusting fermentation. The system described here provided a strong basis for further development of the *E. coli*-produced recombinant EL and its future application for preparation of the mutants and isotope-labelled samples applicable for the deeper structural studies of this amyloid protein.



## Conclusions

- A $\beta$ 40cys2 and A $\beta$ 40cys39 mutant peptides self-assemble to form fibrillar structures, which are similar to fibrils formed by A $\beta$ 40.  $\alpha$ -Syn<sub>141</sub> mutant self-assembles to form fibrils, which have different morphology than  $\alpha$ -Syn fibrils.
- Fibrils formed by  $\alpha$ -Syn<sub>141</sub> can be modified with biotin and gold nanoparticles.
- Hybrid streptavidin-A $\beta$ 40 and streptavidin-hydrophobin-A $\beta$ 40 proteins self-assemble to form fibrillar structures different from A $\beta$ 40 fibrils. Hybrid proteins from PQQ-GDH, A $\beta$ 40 and  $\alpha$ -Syn self-assemble to form very heteromorphic fibrils.
- Hybrid Trx-A $\beta$ 40 protein interacts with heme, moreover, the formed complex acts as a peroxidase. Histidines in A $\beta$ 40 sequence are crucial ligands for heme binding.
- Recombinant equine lysozyme, purified from *E. coli*, self-assemble into ring-shaped fibrillar structures.

## List of publications

### Articles

- Bukauskas V., Strazdienė V., Šetkus A., Bružytė S., Časaitė V., Meškys R. (2009) beta-sheeted amyloid fibril based structures for hybrid nanoobject on solid surfaces. *Interface controlled organic thin films*. Book series: Springer Proceedings in Physics. 129: 61-65.
- Časaitė V., Bružytė S., Bukauskas V., Šetkus A., Morozova-Roche L.A., Meškys R. (2009). Expression and purification of active recombinant equine lysozyme in *Escherichia coli*. *PEDS* 22, 649-654.
- Čepononytė S., Bružytė S., Melvydas V., Servienė E. (2008). Production of heterologous proteins using *S. cerevisiae* expression system. *Biologija* 54, 178–182.
- Bružytė S., Časaitė V., Gasparavičiūtė R., Meškys R. (2008). Investigation of the fusion A $\beta$ 40-Trx proteins interaction with heme. *Biologija* 54, 233–237.
- Šetkus A., Bukauskas V., Pavliuk S., Bružytė S., Časaitė V., Meškys R. (2008). Self assemblage of beta sheeted structures on solid state film for biosensors. *Journal of Surface Science and Nanotechnology*, 7, 491–496.

### Tezės:

- Šetkus A., Bukauskas V., Pavliuk S., Bružytė S., Časaitė V., Meškys R. Self assemblage of beta sheeted structures on solid state film for biosensors. 14 th International Conference on Solid Films and Surfaces, Dublin, Ireland, June 30 - July 4, 2008.
- Šetkus A., Bukauskas V., Meškys R., Bružytė S., Laurinavičius V., Razumienė J. Combined biomolecular and solid state surface structures for chemical detection. Seeing at the Nanoscale VI, 9-11 July 2008 Berlin, Germany.
- Bukauskas V., Šetkus A., Meškys R., Bružytė S. Beta-sheeted amyloid fibril based scaffold structures for development of hybrid nanoobjects with modifyable electronic properties. European Material Research Society 2008 Spring Meeting. Strasbourg, France, May 26-30, 2008.

## **Acknowledgments**

I would like to thank my scientific supervisor dr. Vida Časaitė and the personell of the Department of Molecular Microbiology and Biotechnology, especially Head of the Department dr. Rolandas Meškys, dr. Irina Bachmatova, dr. Liucija Marcinkevičienė, dr. Rasa Rutkienė, dr. Renata Gasparavičiūtė, Virginija Dzekevičienė, Algimantas Krutkis, PhD students: Rūta Stanislauskienė, Jonita Stankevičiūtė, Simonas Kutanovas, Justas Vaitekūnas and Laimonas Karvelis for their assistant and support.

I would like to thank dr. Virginijus Bukauskas and dr. Arūnas Šetkus for help with AFM. I also thank to dr. Juozas Staniulis for help with TEM.

I give thanks to dr. Anders Olofsson, dr. Mantas Mališauskas, dr. Ludmilla Morozova-Roche and dr. Gunter Stier for plasmids.

I would like to thank to PhD students Rimai Budvytytė and Marija Jankunec for assistance with AFM.

I am grateful to dr. Laura Kalinienė for valuable remarks.

I am very grateful to my family and my friends for understanding and support.

This study was partially supported by the Lithuanian State Studies Foundation.

## Santrauka

Savitvarkės biomolekulės, gebančios formuoti  $\beta$ -klostines struktūras, gali būti pritaikomos nanomedžiagų, pasižyminčių naujomis elektrinėmis, optinėmis, katalizinėmis ir/ar mechaninėmis savybėmis, kūrimui. Šiame darbe buvo siekiama kurti nanodarinius, amiloidines fibriles formuojančių baltymų ( $A\beta$ 40,  $\alpha$ -Syn, EL) pagrindu, kurie būtų pagrindas nano dydžio funkcinių sistemų gamybai. Šiam tikslui buvo sukonstruoti mutantiniai ir hibridiniai baltymai bei tiriamos jų suformuotų fibrilinių struktūrų savybės. Sukurti  $A\beta$ 40 ir  $\alpha$ -Syn mutantai, kuriuose genų inžinerijos metodais viena aminorūgštis yra pakeista į Cys. Tokie peptidai gali būti modifikuojami per cisteino tiolinę grupę. Pirmą kartą buvo pademonstruotas  $\alpha$ -Syncys141 fibrilių modifikavimas biotinu ir aukso nanodalelėmis, konjuguotomis su neutravidinu. Taip pat sukonstruoti hibridiniai baltymai, kurie sudaryti iš  $A\beta$ 40 ar  $\alpha$ -Syn bei GDH, streptavidino ir hidrofobino. Buvo tikimasi, kad tokie baltymai formuos fibrilines struktūras, o funkciniai baltymai bus aktyvūs. Šio darbo rezultatai parodė, kad hibridiniai baltymai galėjo formuoti fibriles, kurios labai skyrėsi morfologiškai. Tačiau tik streptavidino ir  $A\beta$ 40 baltymas formavo fibrilinę struktūrą – tinklą, o streptavidinas buvo aktyvus. Šiame darbe pirmą kartą buvo aprašytas ir rekombinantinio kumelės pieno lizocimo (EL) gamyba *E. coli* ląstelėse. Taip pat buvo nustatyta, kad rekombinatinis EL baltymas galėjo formuoti panašias į natyvaus EL fibrilines struktūras. Atlikti eksperimentai ir gauti rezultatai rodo, kad gauti nauji hibridiniai ir mutantiniai baltymai, gebantys formuoti amiloidines fibriles, yra geras pagrindas tolimesniems darbams, kuriant funkcionalizuotus darinius.

## Curriculum vitae

**Name:** Simona Povilonienė (Bružytė)  
**Date and place of birth:** 05.04.1982, Klaipėda  
**Office address:** Vilnius University Institute of Biochemistry,  
Mokslininkų 12  
LT-08662 Vilnius, Lithuania  
**Phone:** (+370 5) 2729149  
**E-mail:** [simona.poviloniene@bchi.vu.lt](mailto:simona.poviloniene@bchi.vu.lt)

**Education:**  
2006 – 2010 Ph. D. studies, Biochemistry, Institute of Biochemistry,  
Vilnius, Lithuania  
2004 – 2006 MSc, Biology (Genetics), Vilnius University, Lithuania  
2000 – 2004 BSc, Biology (Molecular Biology), Vilnius University,  
Lithuania

**Employment:**  
from 2010 Junior research associate, VU Institute of Biochemistry, Vilnius,  
Lithuania  
2006 – 2010 Technician, Institute of Biochemistry, Vilnius, Lithuania  
2003 – 2004 Research assistant, Institute of Biochemistry, Vilnius,  
Lithuania

**Research interests:** Amyloid-forming proteins; catabolism of glycine betaine in  
*Arthrobacter* sp.

### Scientific publications:

1. Časaitė V., Bružytė S., Meškys R. (2004). Analysis of transcription of dimethylglycine oxidase operon from *Arthrobacter globiformis*. *Biologija* 2:50-53.
2. Časaitė V., Bružytė S., Meškys R. (2006). Effect of glycine betaine on osmoadaptation of *Arthrobacter* strains. *Biologija* 4:46–48.
3. Bružytė S., Časaitė V., Gasparavičiūtė R., Meškys R. (2008). Investigation of the fusion Trx-Aβ40 proteins interaction with heme. *Biologija*, 54(4): 233-237.
4. Čepononytė S., Bružytė S., Melvydas V., Servienė E. (2008). Production of heterologous proteins using *S. cerevisiae* expression system. *Biologija*, 54(3): 178-182.
5. Časaitė V., Bružytė S., Bukauskas V., Šetkus A., Morozova-Roche L.A., Meškys R. (2009). Expression and purification of active recombinant equine lysozyme in *Escherichia coli*. *PEDS* 22: 649-654.
6. Šetkus A., Bukauskas V., Pavliuk S., Bružytė S., Časaitė V., Meškys R. (2009). Self assemblage of beta sheeted structures on solid state film for biosensors. *e-Journal of Surface Science and Nanotechnology* 7, 491-496.
7. Bukauskas V., Strazdienė V., Šetkus A., Bružytė S., Časaitė V., Meškys R. (2009). beta-sheeted amyloid fibril based structures for hybrid nanoobject on solid surfaces. *Interface controlled organic thin films*. Book series: Springer Proceedings in Physics. 129: 61-65.
8. Časaitė V., Povilonienė S., Meškienė R., Rutkienė R., Meškys R. (2011). Studies of dimethylglycine oxidase isoenzymes in *Arthrobacter globiformis* cells. *Curr Microbiol* 62(4):1267-73.